

Measuring the dynamical properties of self-gravitating systems in their outer regions through the caustic technique

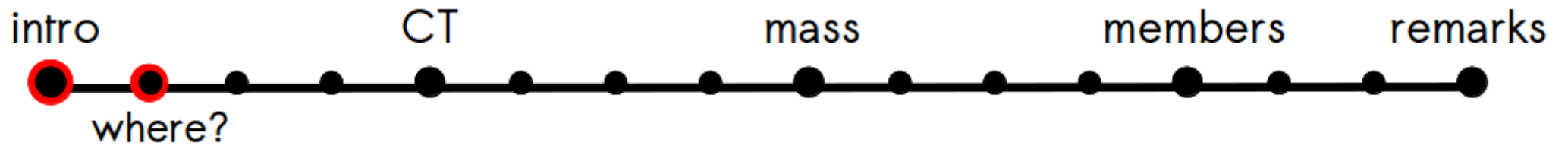
Ana Laura Serra



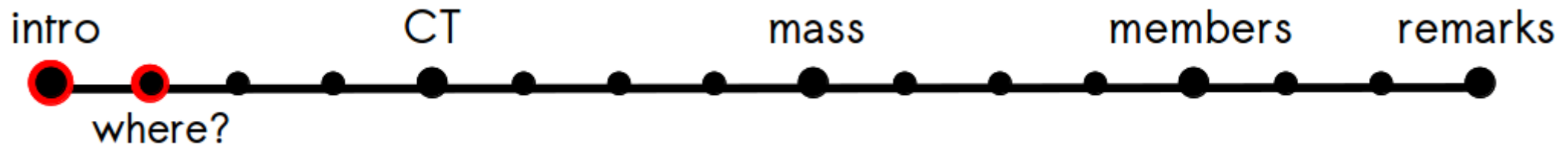
CAUSTIC Group
Dipartimento di Fisica
Università di Torino



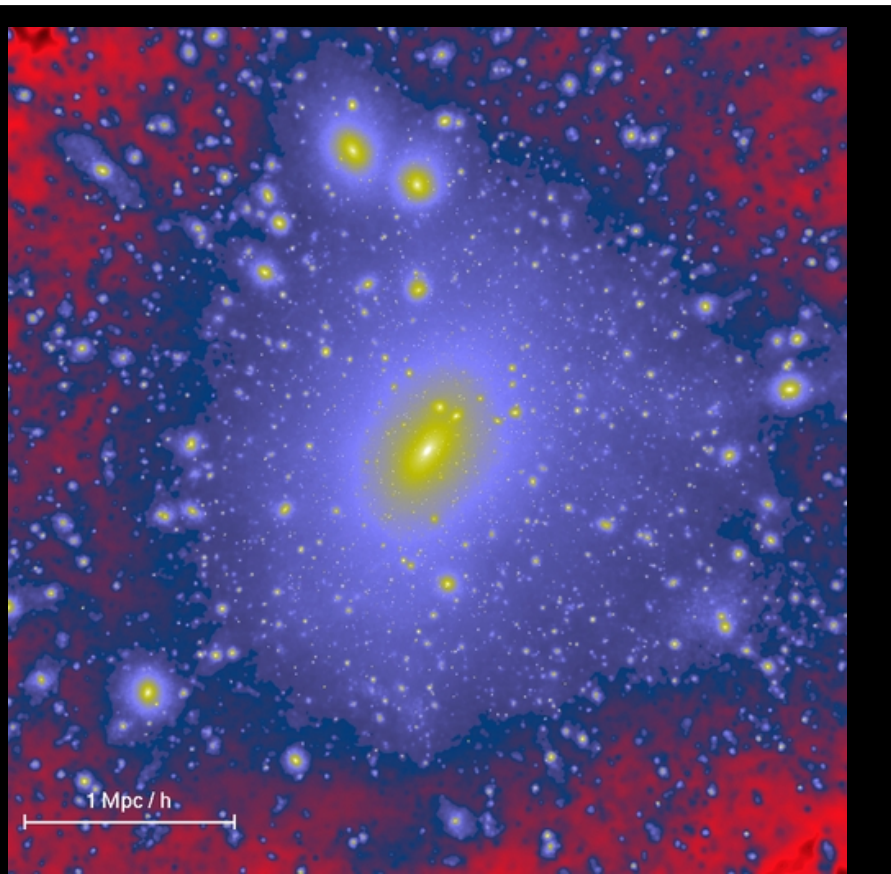
Trieste, September 26th, 2012



Abell 1689 observed by the Hubble Space Telescope



Formation of large-scale structure in the Universe



Millennium Simulation, Volker Springel, 2005

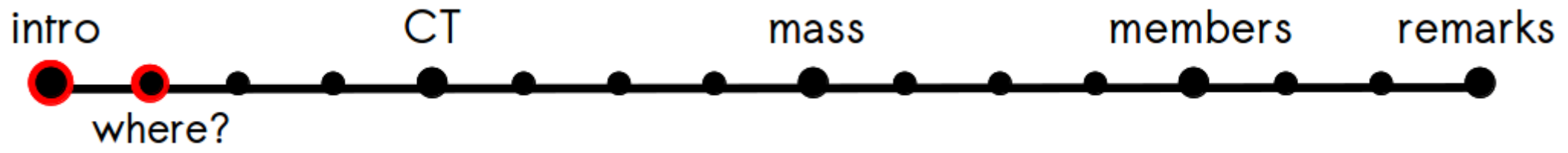


Early Universe
(small perturbations)

ripples evolve independently

they interact with others in non-linear ways

the small over-density fluctuations attract additional mass as the Universe expands

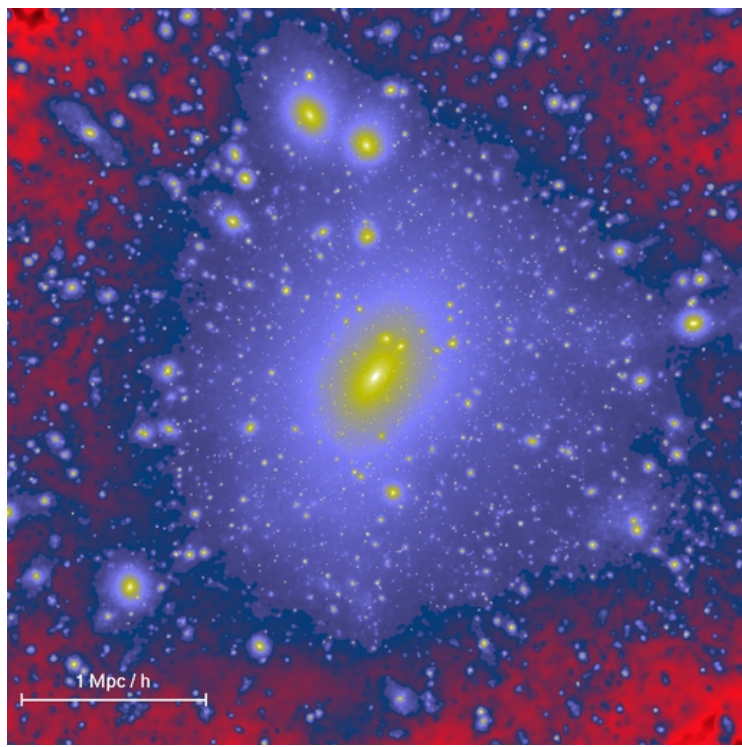


Formation of large-scale structure in the Universe

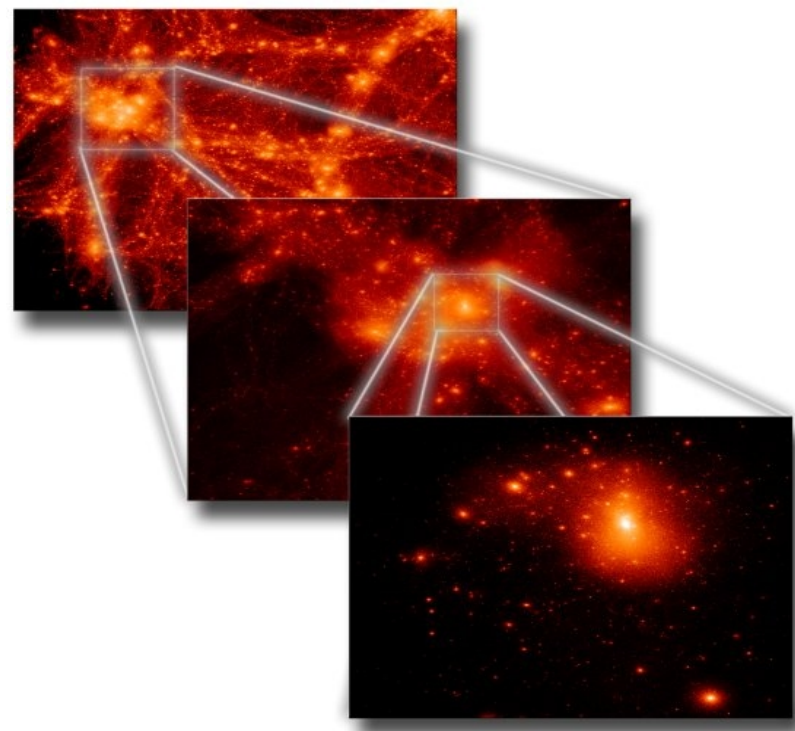
Gravitational instability produces high peaks of the density field



merger of small clumps at the intersection of a filamentary large-scale structure



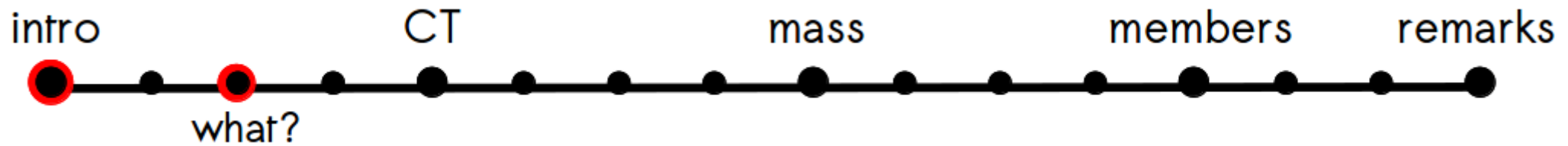
Millennium Simulation, Volker Springel, 2005



Simulation by Gauss Centre for Supercomputing
Gottlöber, Khalatyan, Klypin, 2008



GALAXY CLUSTER



cosmological **large-scale** *nucleosynthesis*
structure **galaxy-environment**
 galaxy formation **matter distribution**

~80% - DM
 ~20% - hot diffuse plasma
 - stars, dust, cold gas

parameters —————

largest gravitationally bound systems in the Universe

a few Mpc
 $\sim 10^{14-15} M_{\text{sun}}$

hundreds of galaxies

galaxy-environment connection

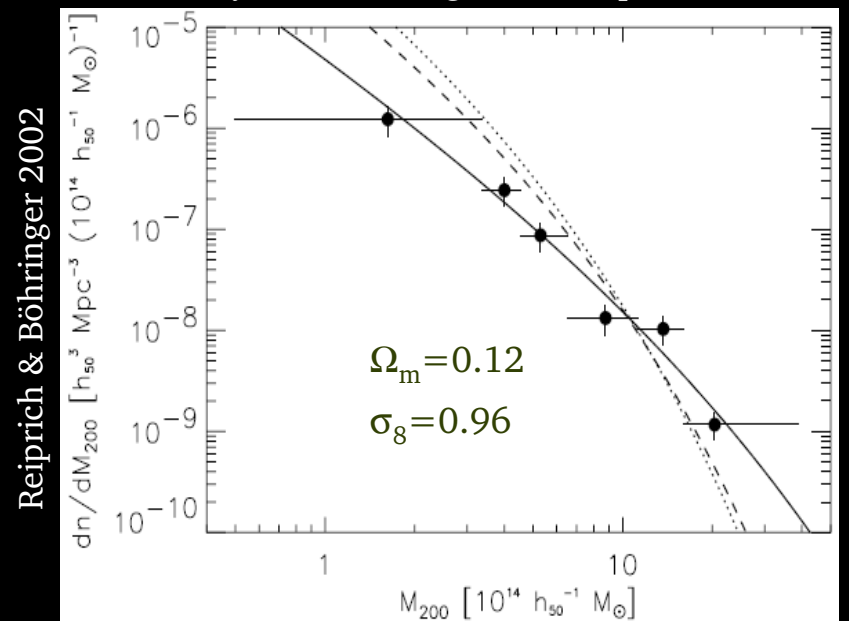


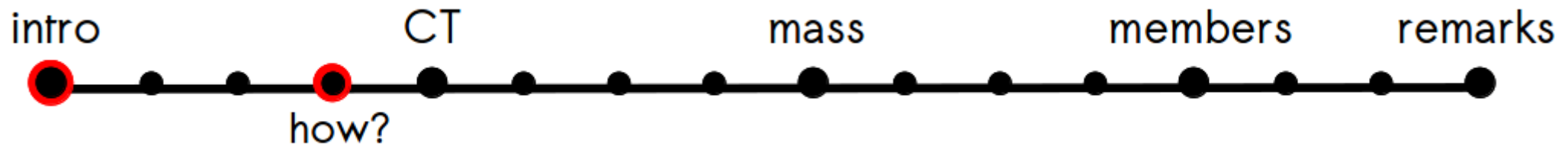
High-mass tail of mass function

↓
number density

↓
 measurement of cosmological parameters

number of systems with a given mass per unit volume





mass distribution

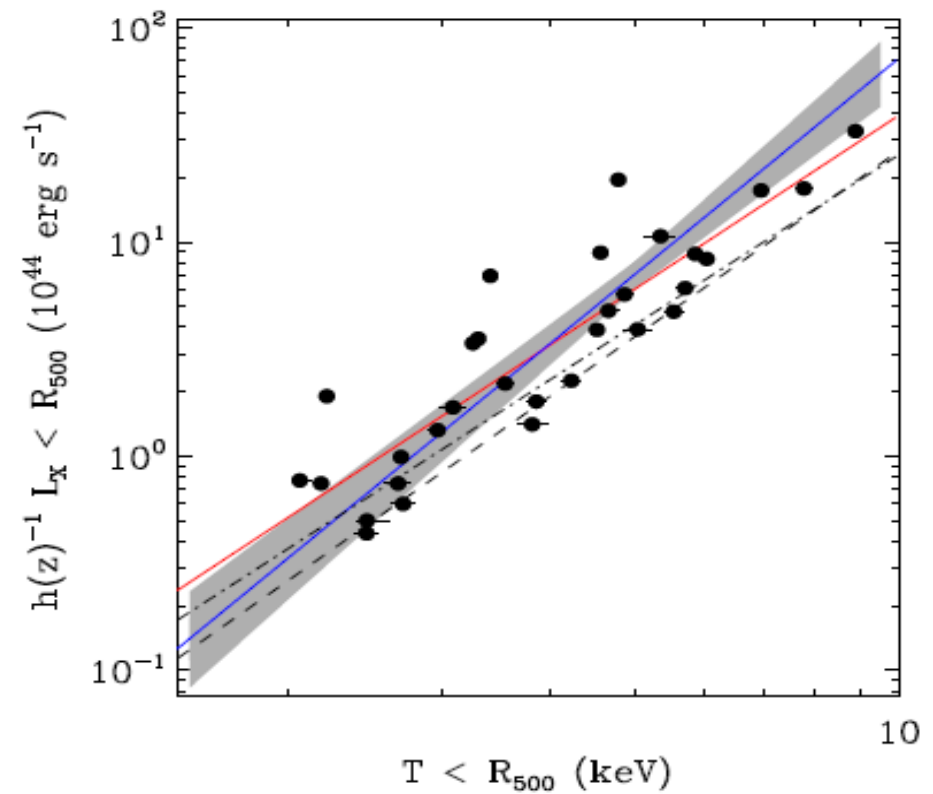
small scales → assumption of dynamical equilibrium

Intermediate scales (1-10 Mpc/h)

large scales → small overdensities → linear theory

can we assume dynamical equilibrium?

from scaling relations... ~yes

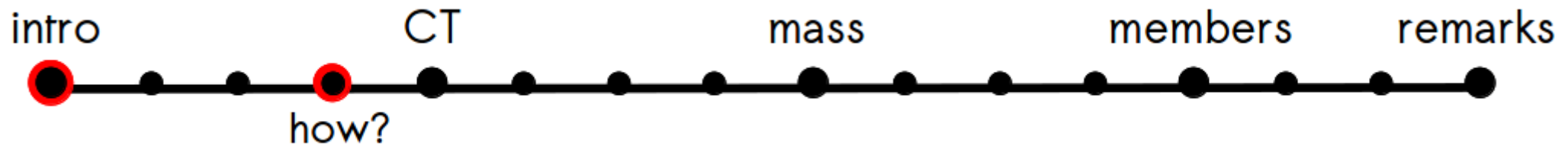


Pratt et al. 2009

however there are...

spatially inhomogeneous thermal and non thermal emission

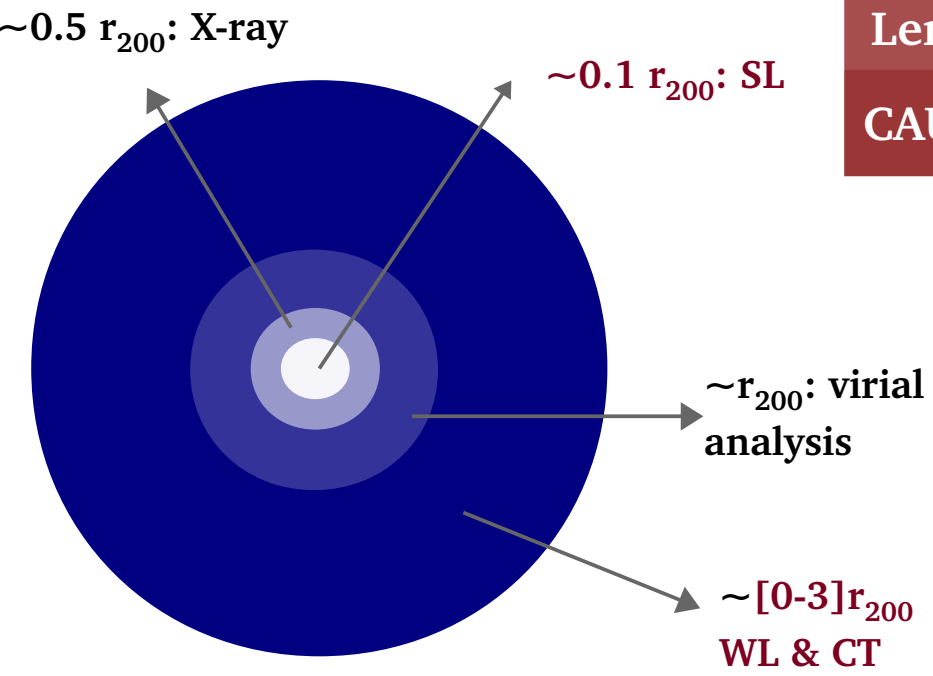
kinematic and morphological segregation of galaxies



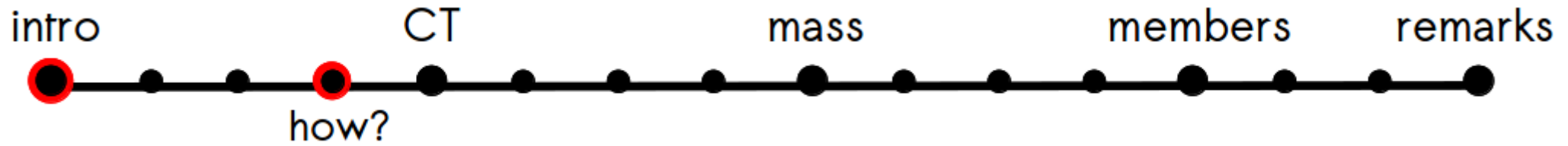
how to measure the mass of galaxy clusters ?

- Virial theorem
- Jeans Equation
- Scaling relations
- X-ray temperature
- Strong and Weak Lensing
- CAUSTIC TECHNIQUE

No assumption of dynamical equilibrium



r_{200} : radius enclosing a matter density 200 times the critical density of the Universe $\sim 277.5 h^2 M_{\odot} / \text{Mpc}^3$



total mass within a radius

mass profile

from l.o.s. velocities and position

virial theorem

$$M = \frac{3\sigma^2 R}{G}$$

$$R = \frac{\pi N(N-1)}{2} \left(\sum_i \sum_{i>j} \frac{1}{r_{ij}} \right)^{-1}$$

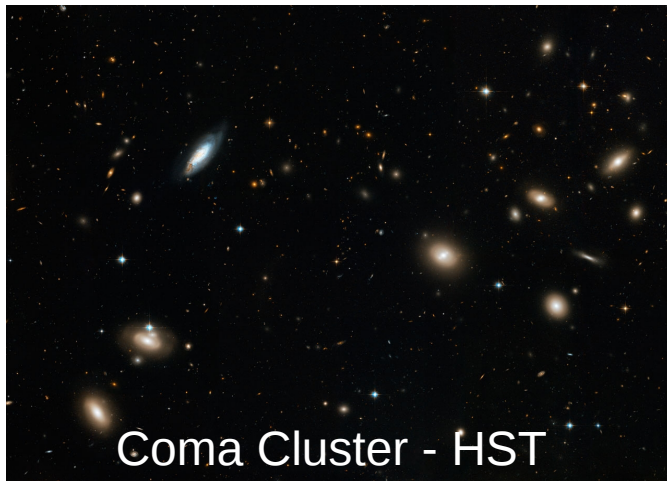
Jeans equation

$$M(< r) = \frac{\langle v_r^2 \rangle r}{G} \left[\frac{d \ln \rho_m}{d \ln r} + \frac{d \ln \langle v_r^2 \rangle}{d \ln r} + 2\beta(r) \right]$$

$$\beta(r) = 1 - \frac{\langle v_\theta^2 \rangle + \langle v_\phi^2 \rangle}{2\langle v_r^2 \rangle}$$

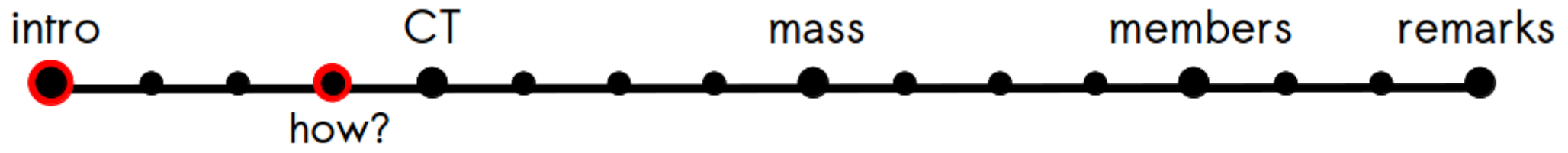
scaling relations

mass-anisotropy degeneracy
 assumption of relation between the
 galaxy density profile and the
 mass density profile



Coma Cluster - HST

dynamical equilibrium + sphericity



total mass within a radius

mass profile

from X-ray

X-ray temperature

isothermal ICM → important departure from assumption in some clusters

scaling relations

the complex thermal structure of the ICM can bias the estimate.

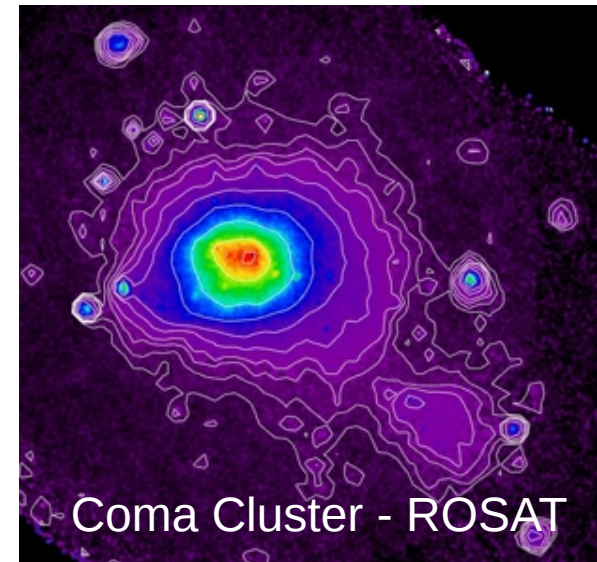
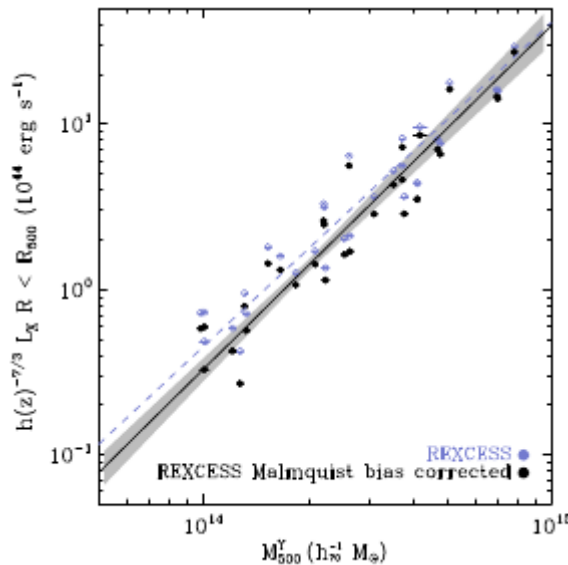
X-ray spectrum

$$M(< r) = \frac{kTr}{G\mu m_p} \left[\frac{d \ln \rho_{gas}}{d \ln r} + \frac{d \ln T}{d \ln r} \right]$$

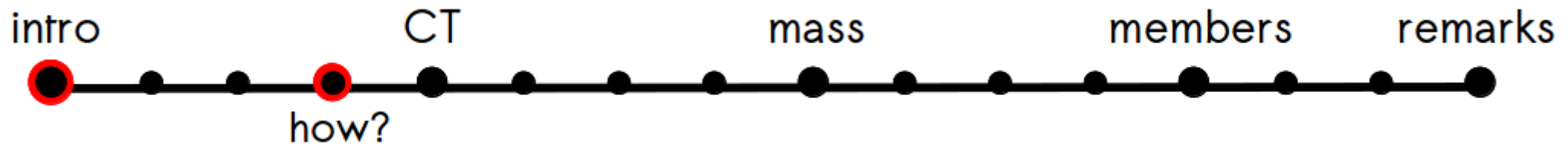
no β → the ICM pressure is isotropic

dynamical equilibrium + sphericity

Pratt et al. 2009



Coma Cluster - ROSAT



total mass within a radius

mass profile

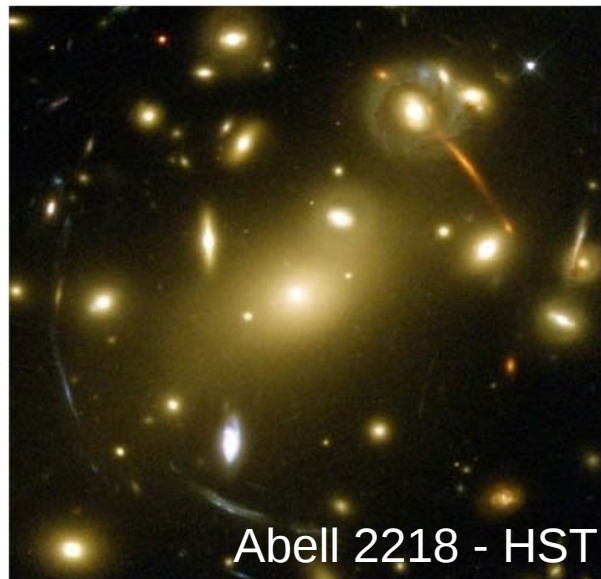
from lensing signal

Strong lensing
 multiple images, arcs

$$M(< r) = \frac{rc^2}{4G} \alpha$$

Weak lensing
 tangential distortion of the shape of galaxies

disadvantage: the signal intensity depends on the distances between observer, lens and source



Abell 2218 - HST

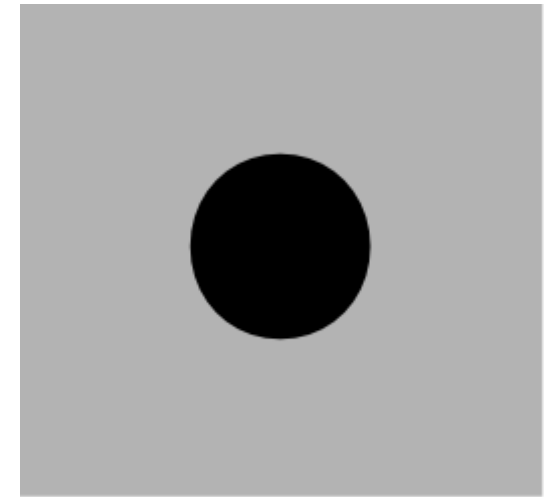
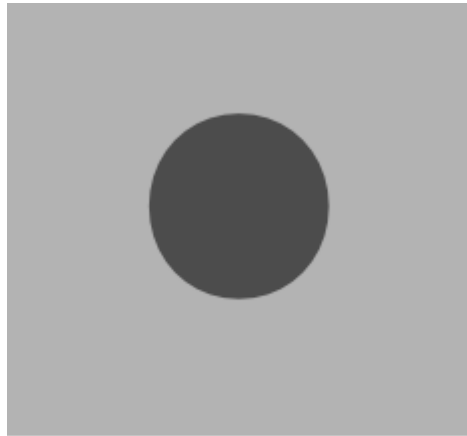
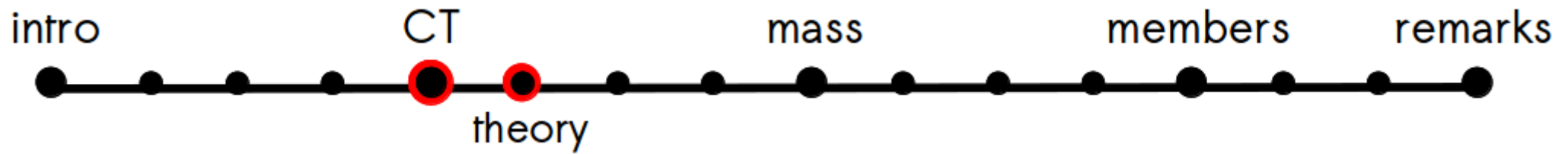
from l.o.s. velocities and position

Caustic technique
 in hierarchical models of structure formation, the velocity field surrounding the cluster is not perfectly radial, as expected in the spherical infall model

↓

it is possible to extract the escape velocity of galaxies from the redshift diagram

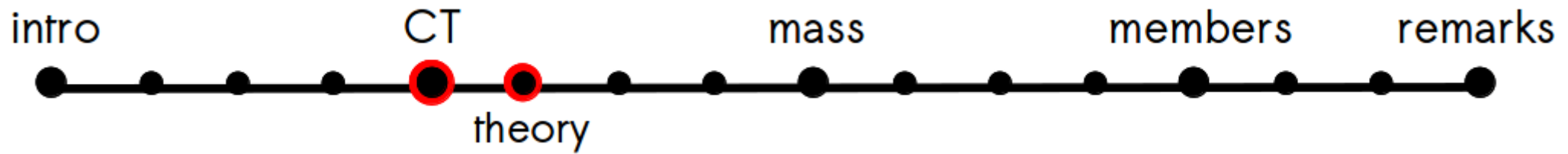
~~dynamical equilibrium + sphericity~~



evolves like a Friedmann model (expanding medium)

for any small density perturbation there will be a competition between its self-gravity (which is attempting to increase the density) and the general expansion of the universe (which decreases the density)

structures will be formed if, at some time, the spherical region ceases to expand with the background universe and begins to collapse

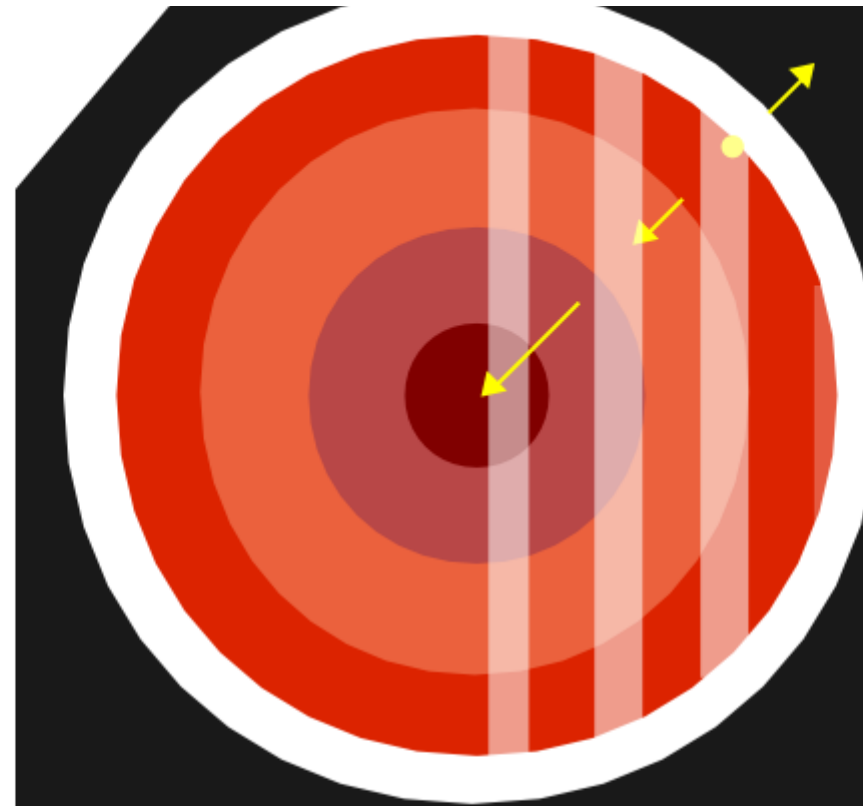


When observed in redshift space, the infall pattern around a rich cluster appears as a “trumpet” whose amplitude $\mathcal{A}(\theta)$ decreases with θ (Kaiser, 1987)

from spherical infall model

(Regös & Geller, 1989)

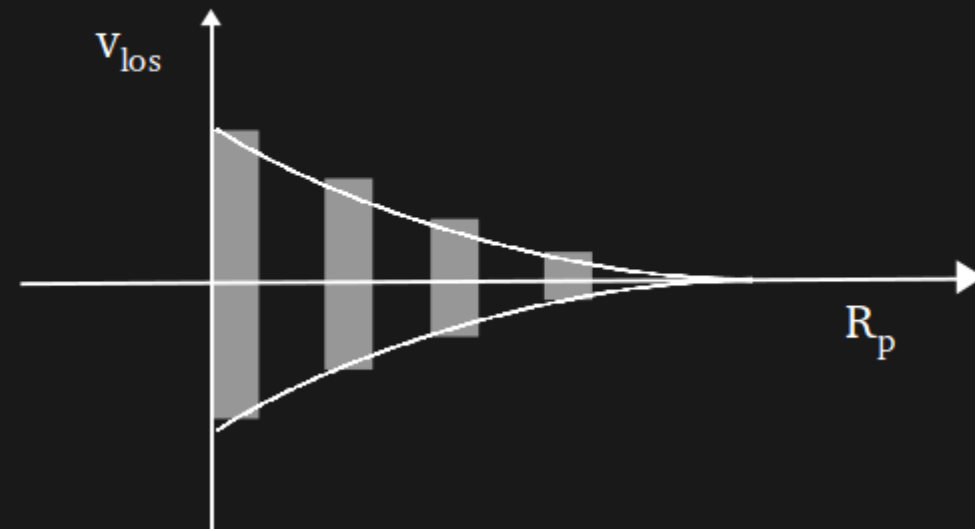
$$\mathcal{A}(\theta) \sim \Omega_0^{0.6} r f(\delta) \sqrt{-\frac{d \ln f(\delta)}{d \ln r}}$$

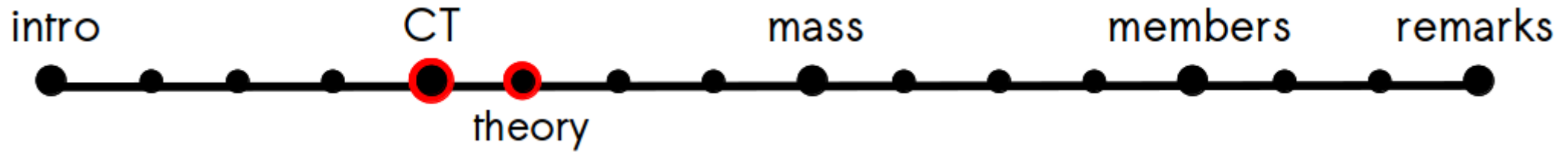


$$\mathbf{v} = H_o \mathbf{r} + \mathbf{v}_{pec}$$

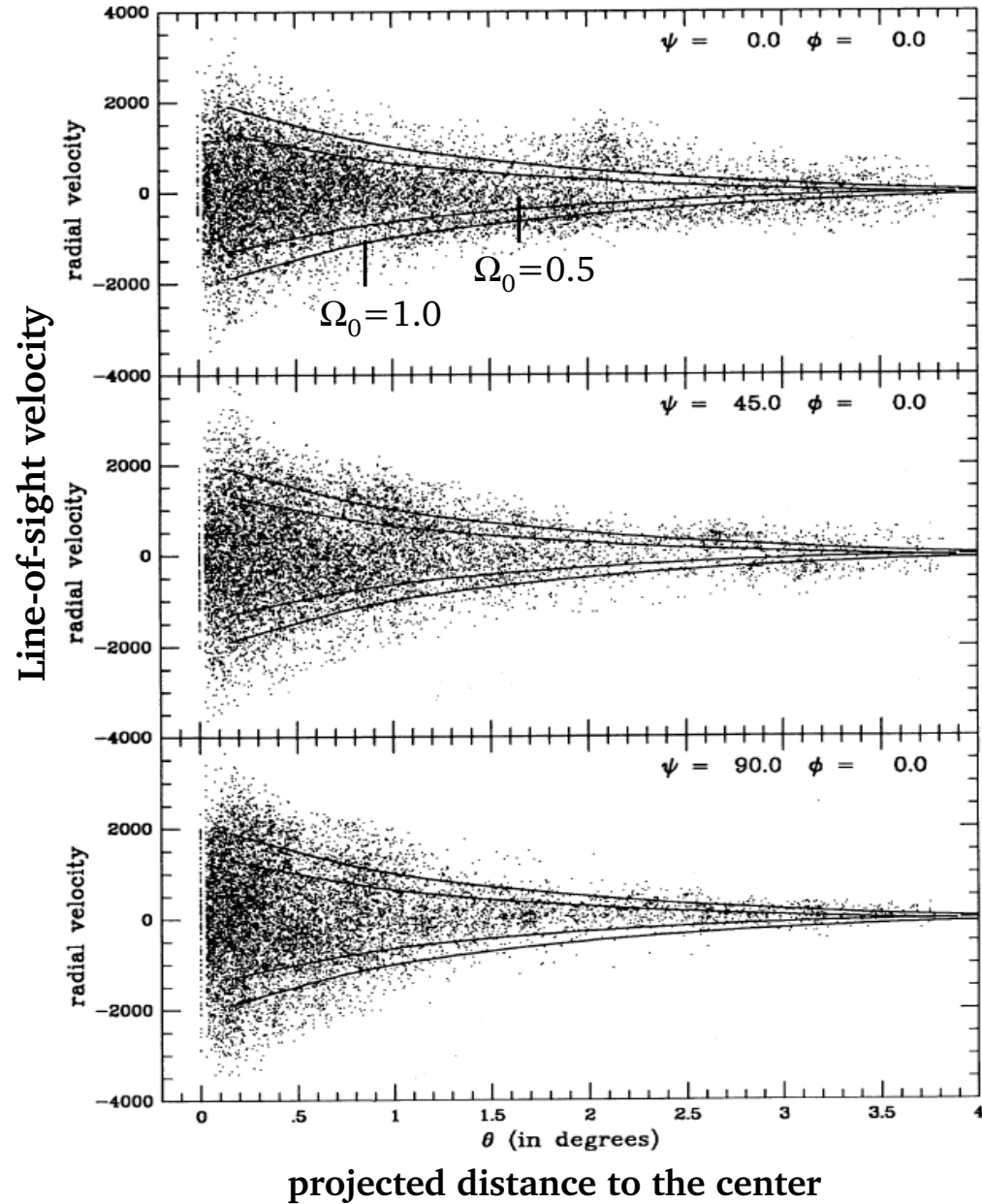
$$v_{turn} = H_o r$$

$$v_{inf} = H_o r - v_{pec}$$

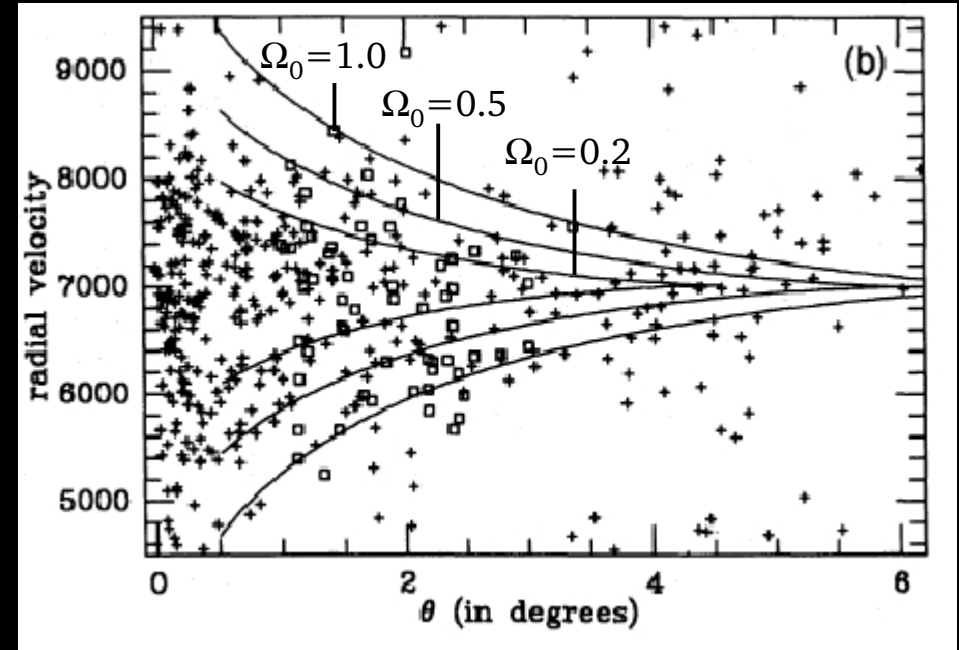




Simulated data

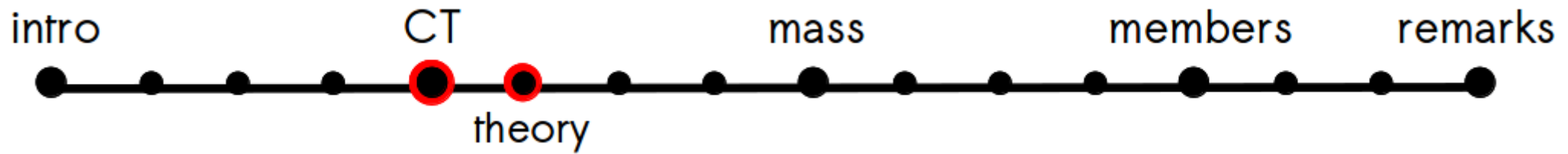


Real data Coma cluster

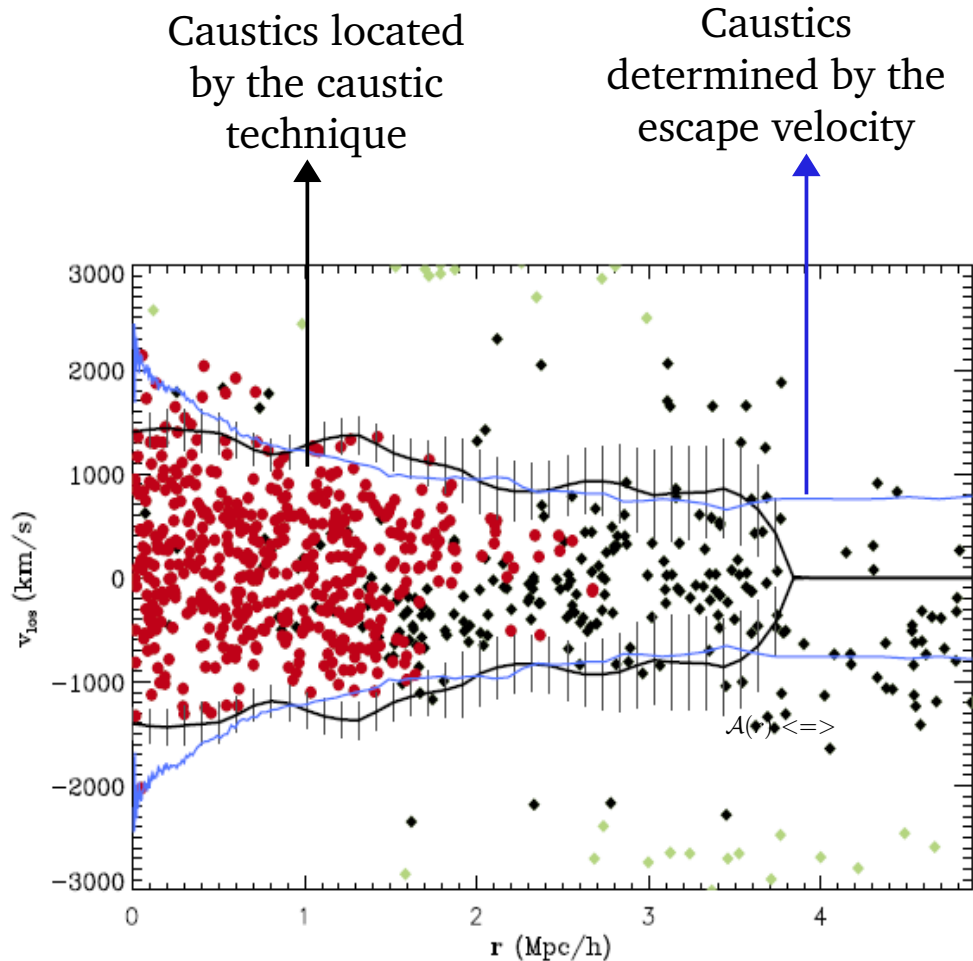


van Haarlem et al. 1993

but clusters accrete mass anisotropically
 → the velocity field can have a substantial non-radial random component



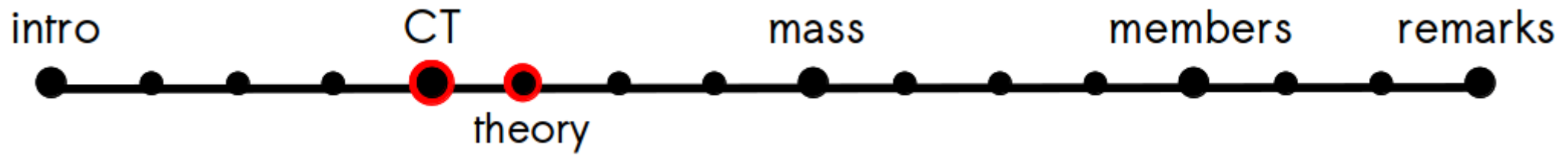
$A(r) \Leftrightarrow$ escape velocity



The random components increase the caustic amplitude when compared to the spherical model

$$A_{\text{infall model}} < A_{\text{non-radial}}$$

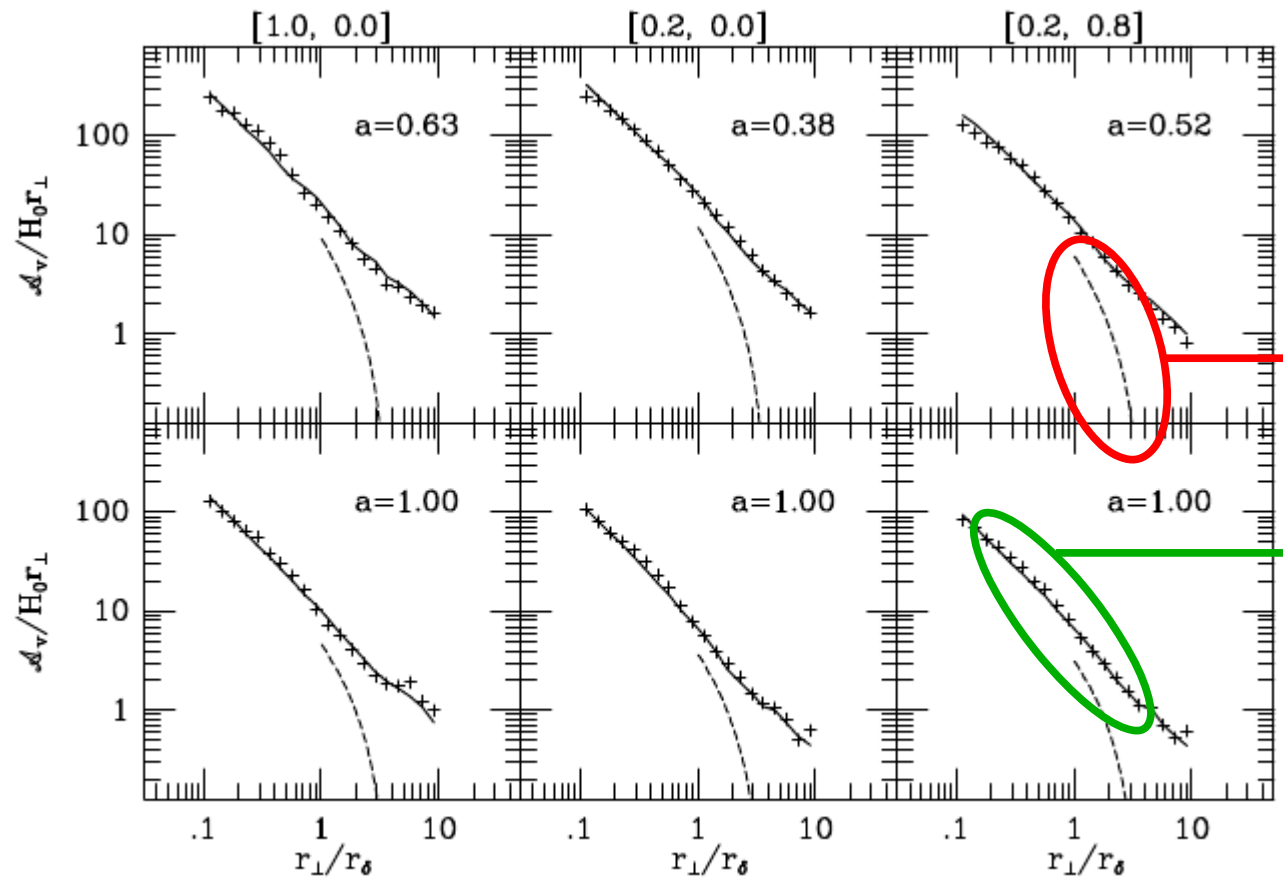
but clusters accrete mass anisotropically
 \rightarrow the velocity field can have a substantial non-radial random component



$A(r) \iff$ escape velocity

flat with ρ_c open flat with low ρ

caustic amplitude



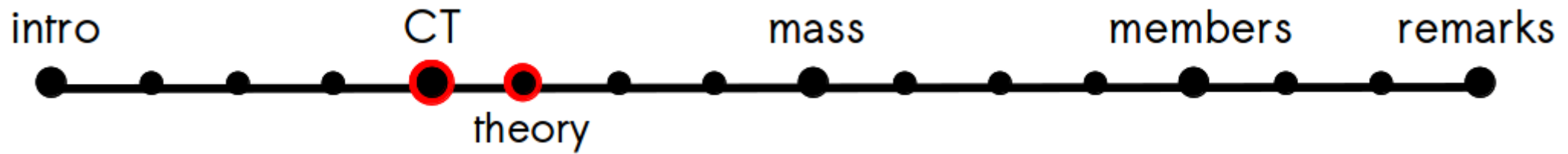
out of equilibrium

spherical infall model

caustic amplitude

in equilibrium

radius



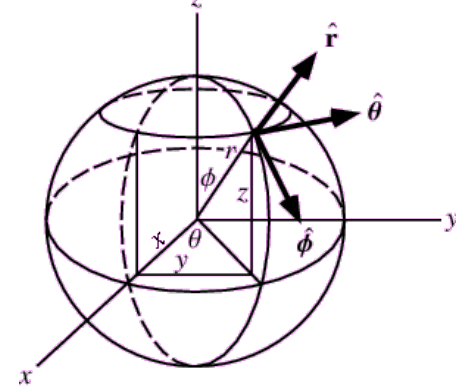
Interpretation: $\mathcal{A}(\theta)$ is the average over a volume $d^3\mathbf{r}$ of the square of the l.o.s. component of the escape velocity

$$\mathcal{A}^2(r) = \langle v_{esc,los}^2 \rangle$$

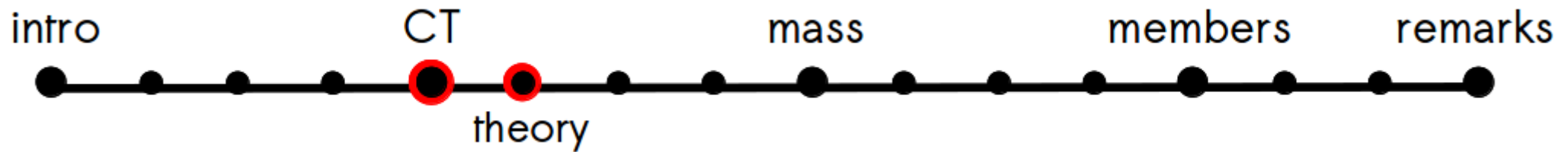
$$\langle v_{esc,los}^2 \rangle = -2\phi(r)g^{-1}(\beta)$$

$$\beta(r) = 1 - \frac{\langle v_{\theta}^2 \rangle + \langle v_{\phi}^2 \rangle}{2\langle v_r^2 \rangle}$$

HOLDS INDEPENDENTLY OF THE DYNAMICAL STATE OF THE CLUSTER



$$A_{infall\ model} < A_{non-radial}$$



Mass estimate

$$A^2(r) = \langle v_{esc,los}^2 \rangle$$

$$\langle v_{esc,los}^2 \rangle = -2\phi(r)g^{-1}(\beta)$$

mass of an infinitesimal shell

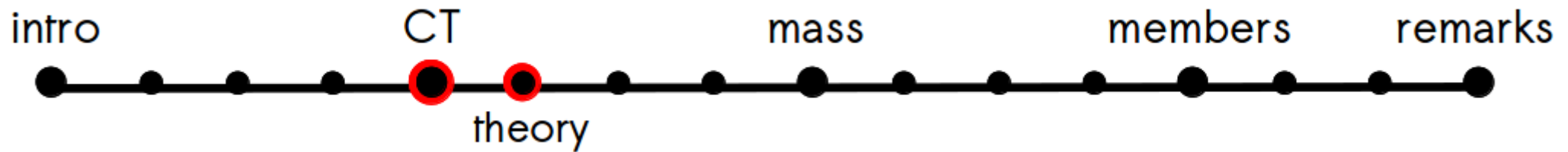
$$G dm = -2\phi(r)\mathcal{F}(r) dr = A^2(r)g(\beta)\mathcal{F}(r) dr$$

where $\mathcal{F}(r) = \frac{-2\pi G\rho(r)r^2}{\phi(r)}$ and

$\mathcal{F}_\beta(r) = \mathcal{F}(r)g(\beta)$ is a slowly changing function of r

theoretical framework of the
CAUSTIC TECHNIQUE

$$GM(< r) = \mathcal{F}_\beta \int_0^r A^2(r) dr$$



Developed in the '90s
(Diaferio & Geller, 1997;
Diaferio, 1999)
Problem: it requires
hundreds of galaxy
redshifts

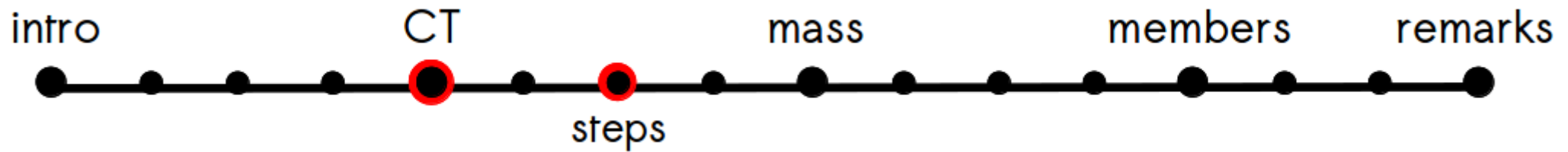
nowadays the
required data are
easily collectable

CAUSTIC TECHNIQUE

Can be applied for

- MASS/POTENTIAL ESTIMATES
- IDENTIFICATION OF MEMBERS
- [IDENTIFICATION OF SUBSTRUCTURES]

to **simulated** and **real** data



1

arrange the galaxies in a binary tree according to a hierarchical method

2

select two thresholds to cut the tree: the largest group obtained from the upper-level threshold identifies the cluster candidate members

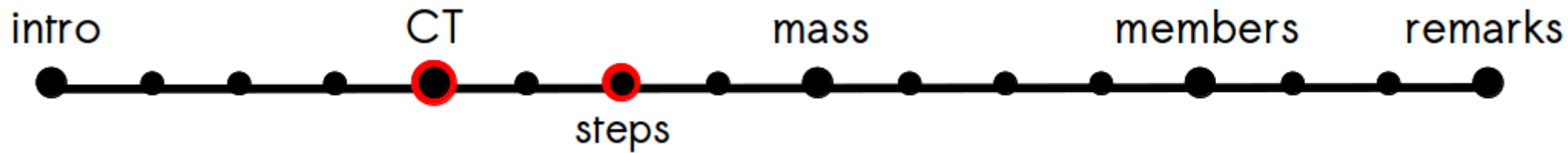
3

build the redshift diagram of all the galaxies in the field; locate the caustics, and identify the final cluster members

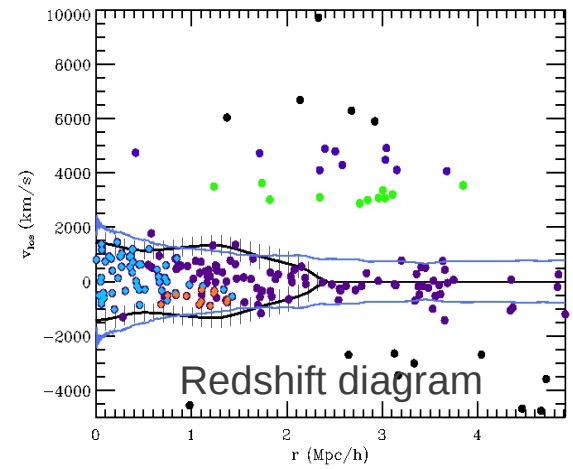
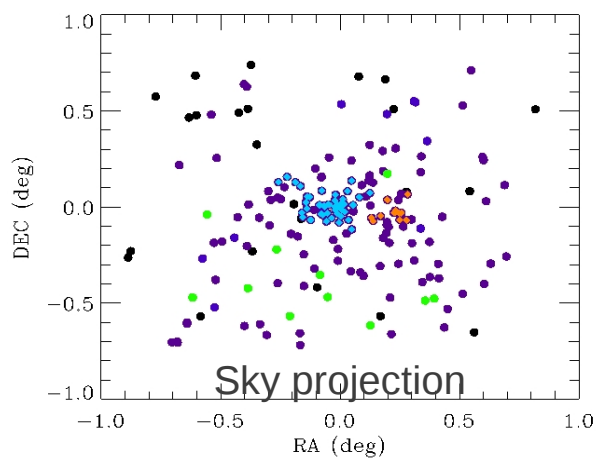
4

the caustic amplitude determines the escape velocity and mass profiles

four steps



1 Binary tree & σ -plateau

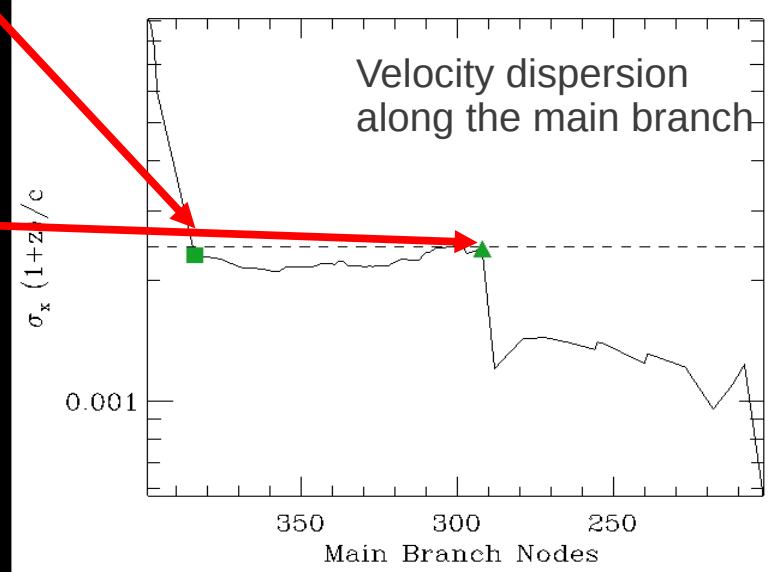
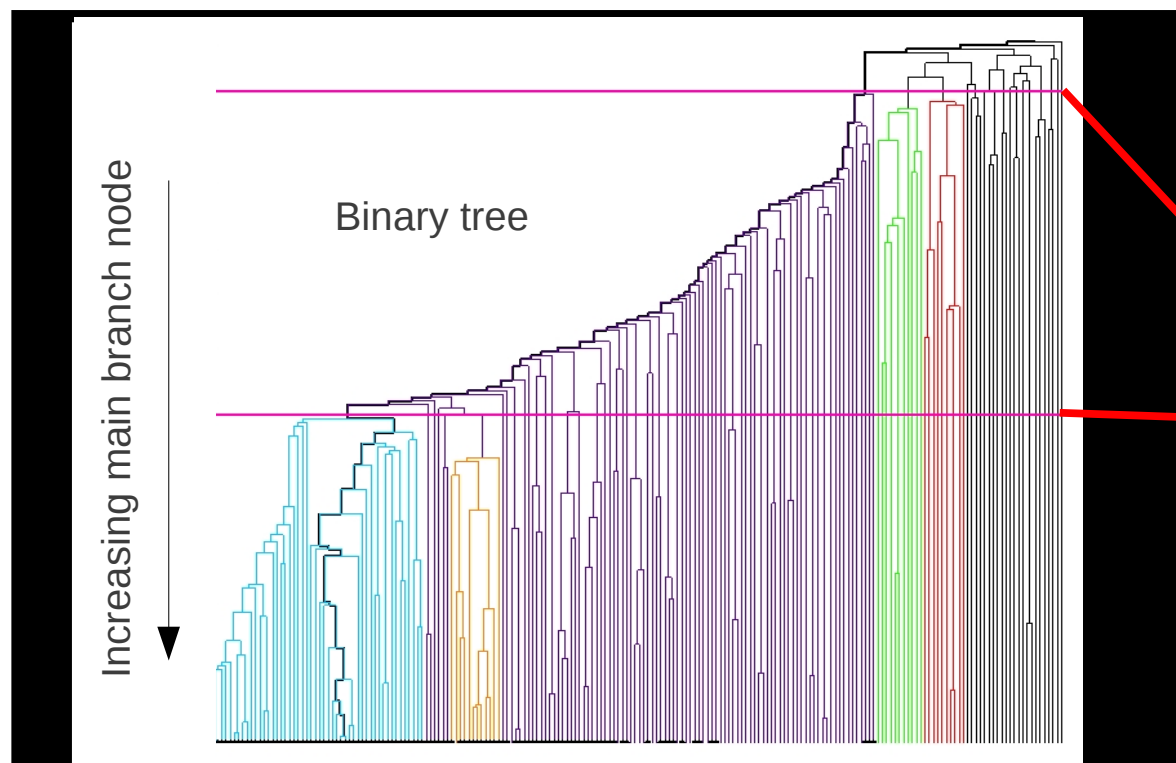


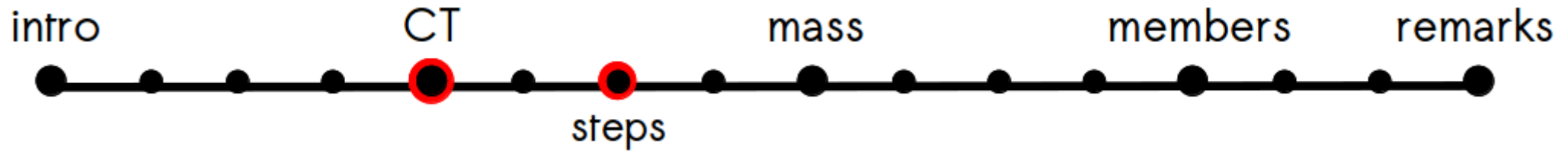
binding energy

$$E_{ij} = -G \frac{m_i m_j}{R_p} + \frac{1}{2} \frac{m_i m_j}{m_i + m_j} \Pi^2$$

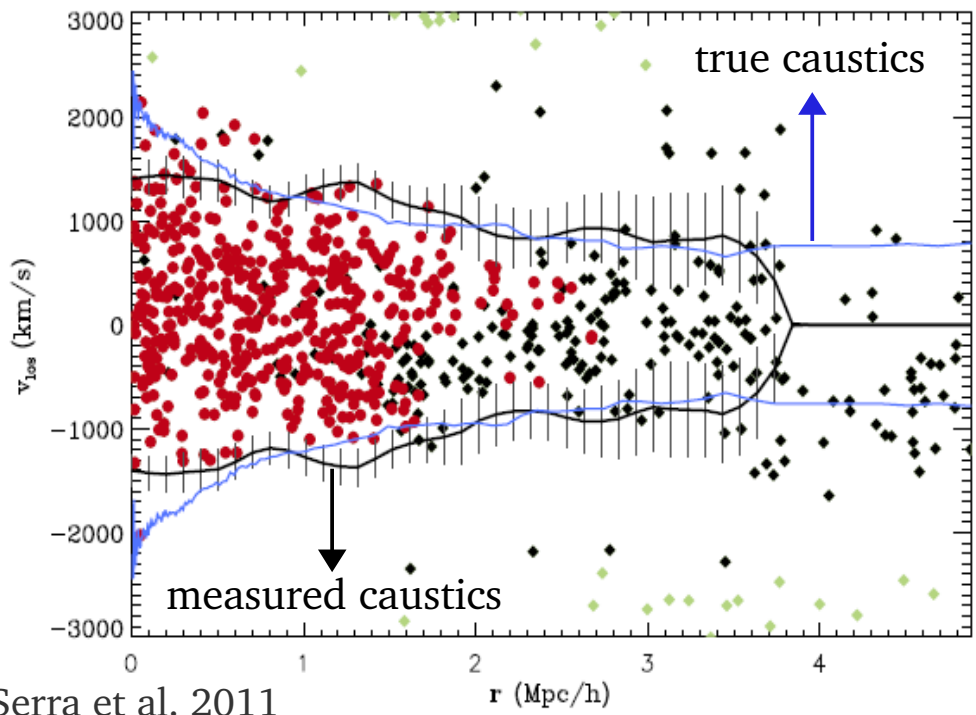
Binary Tree

- σ plateau
- main group members
- size R, center

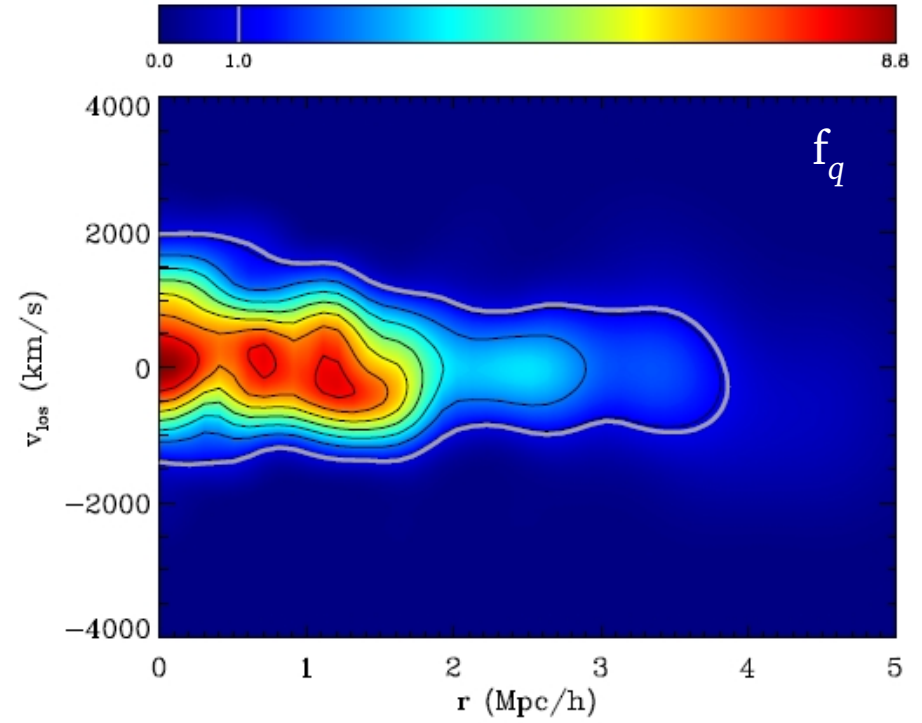




2 Redshift diagram



Serra et al. 2011



3 Caustic location

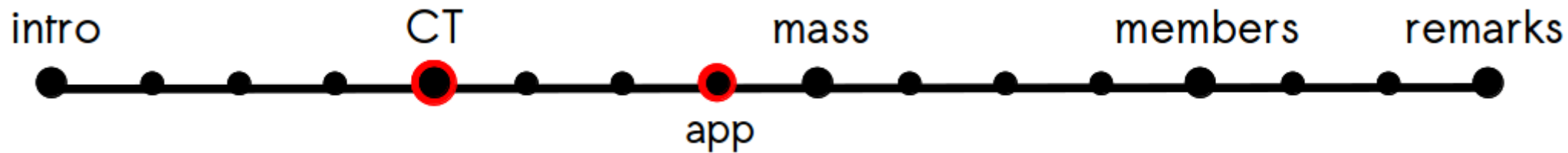
we choose the parameter κ that determines the correct caustic location as the root of the equation

$$S(\kappa) \equiv \langle v_{\text{esc}}^2 \rangle_{\kappa, R} - 4 \langle v^2 \rangle = 0$$

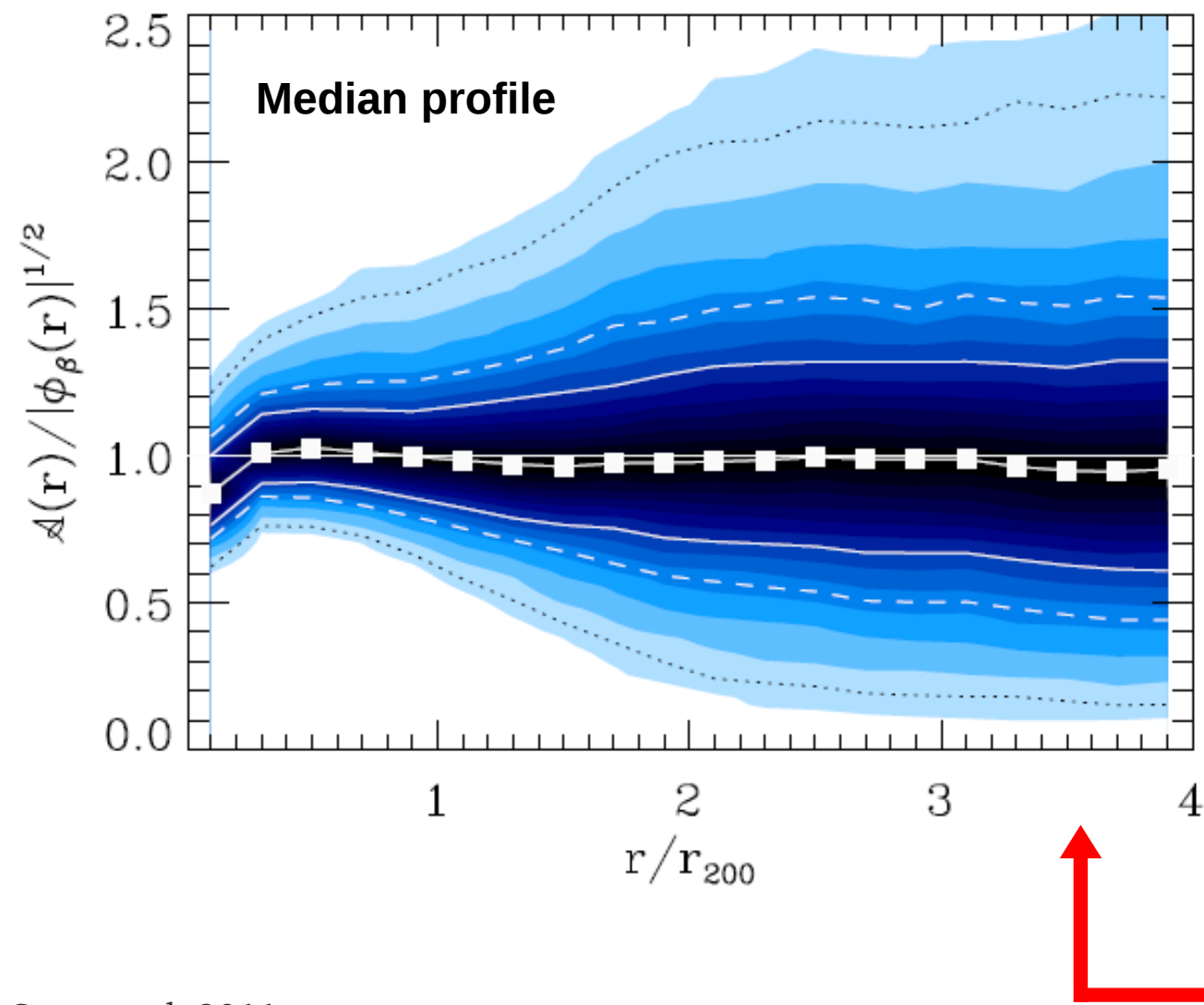
distribution of N galaxies

$$f_q(\mathbf{x}) = \frac{1}{N} \sum_{i=1}^N \frac{1}{h_i^2} K \left(\frac{\mathbf{x} - \mathbf{x}_i}{h_i} \right)$$

$$\mathbf{x} = (r, v)$$

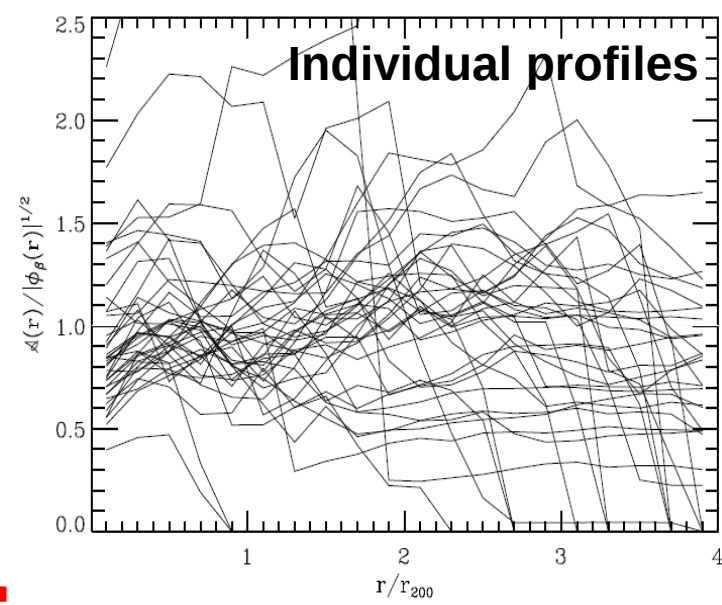


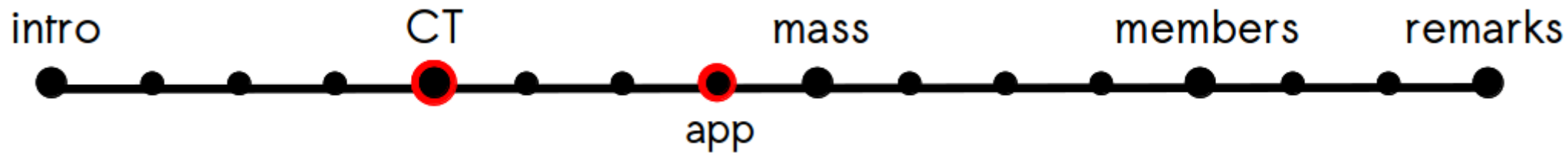
3 Gravitational potential profiles



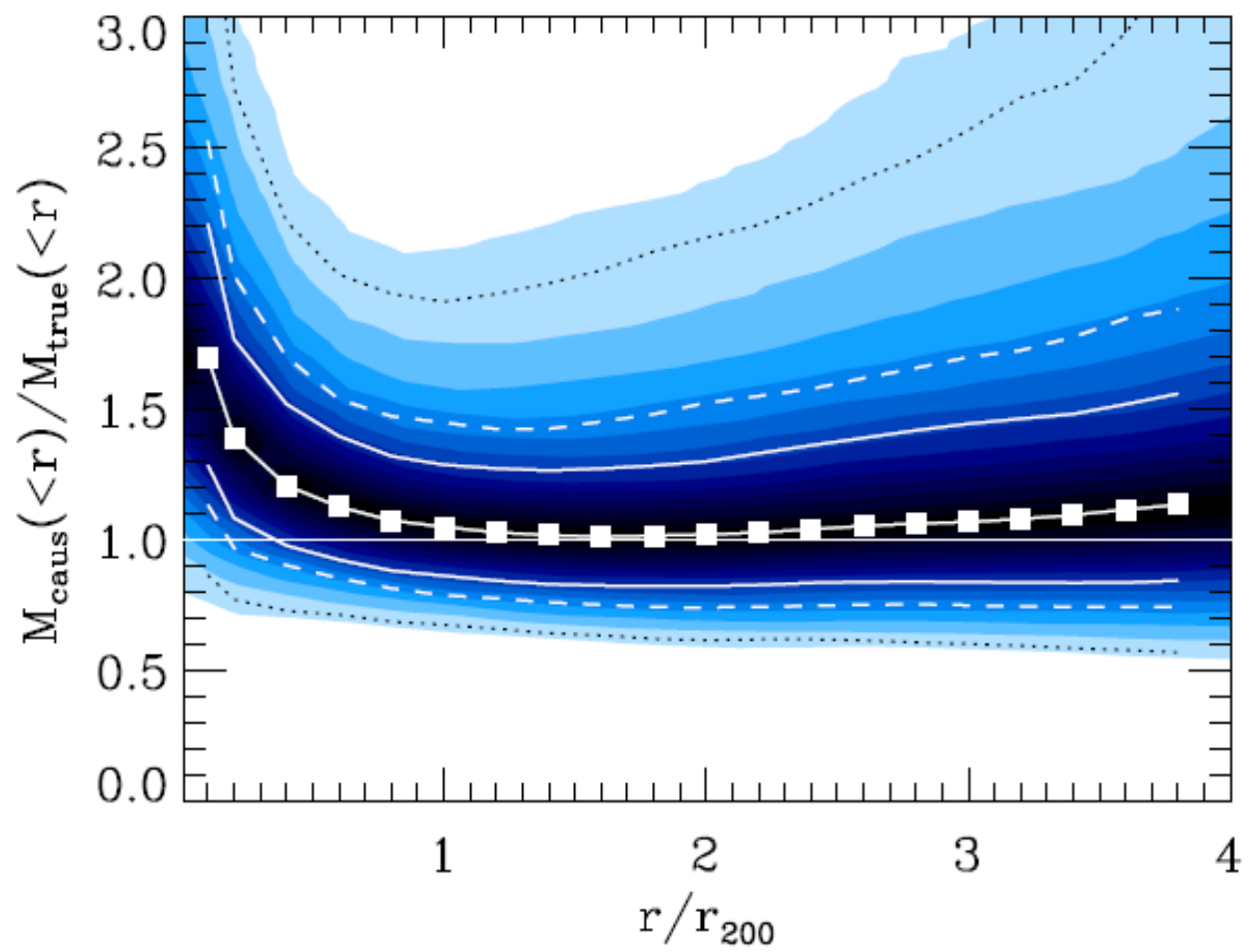
Escape velocity: better than 10% up to $r \sim r_{200}$

3000 simulated clusters with $M_{200} \geq 10^{14} h^{-1} M_\odot$
 from simulation by Borgani et al. 2004



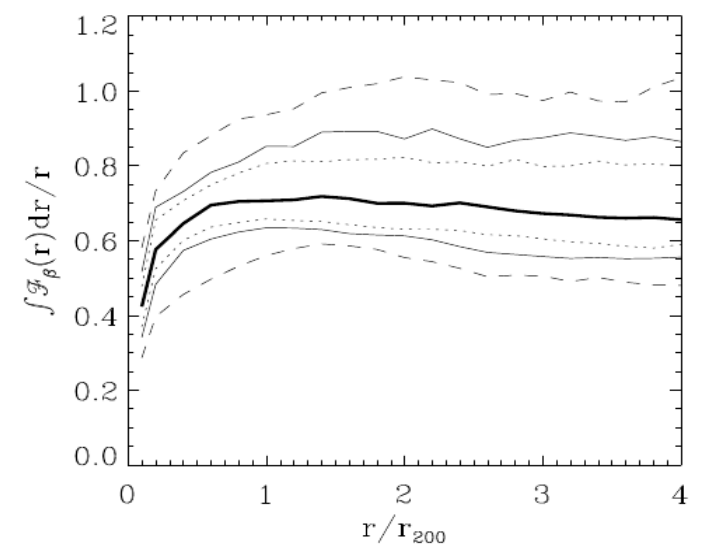


4 Mass profiles



- (0.6-4) $r_{200} \rightarrow$ better than 15%
- $r < 0.6 r_{200} \rightarrow$ overestimation of the mass up to 70%

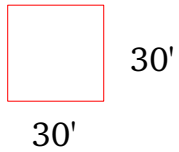
3000 simulated clusters with $M_{200} \geq 10^{14} h^{-1} M_{\odot}$



$$GM(<r) = \mathcal{F}_{\beta} \int_0^r \mathcal{A}^2(r) dr$$

Stacked cluster

$$|v_{\text{los}}^x - v_{\text{los}}^{\text{clus}}| = 2000 \text{ km/s}$$



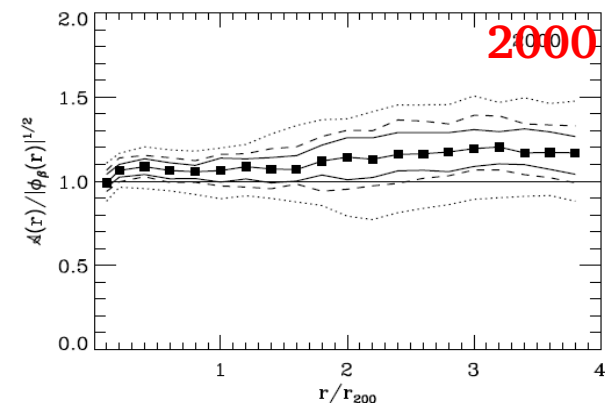
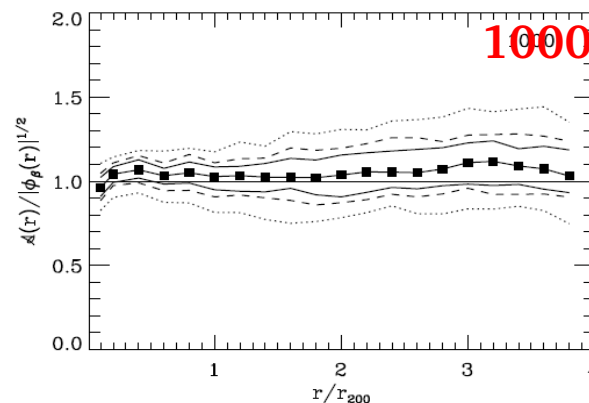
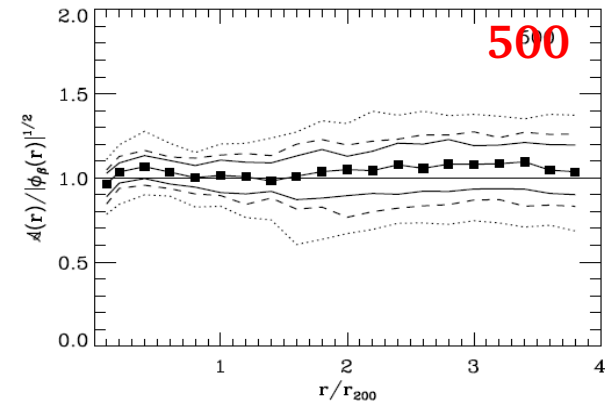
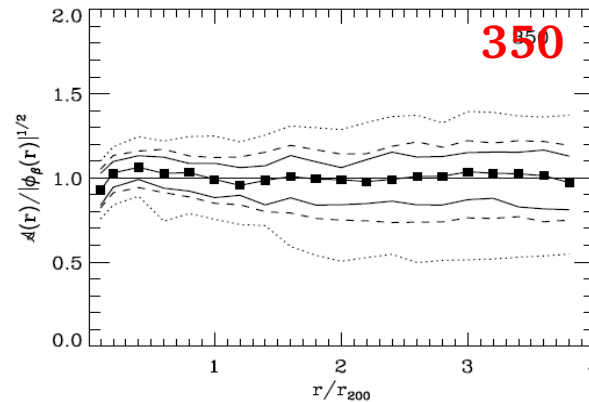
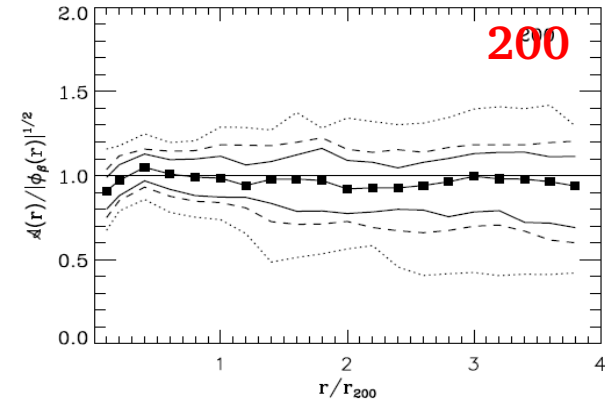
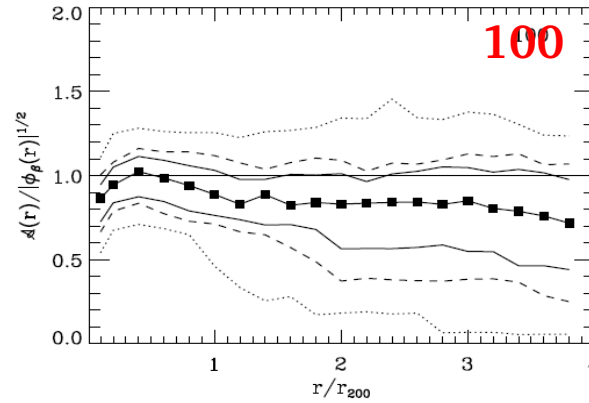
$$z^{\text{clus}} = 0.1$$

$$30' \rightarrow 2.46 \text{ Mpc/h}$$

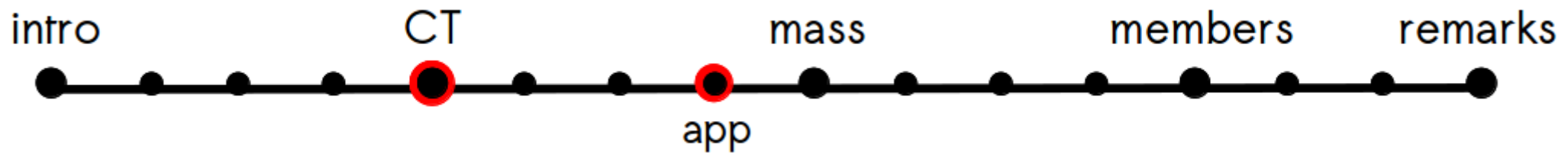
spread decreases with increasing number of galaxies

app

measured caustic amplitude/true caustic amplitude



projected distance to the center



Applications to real systems

Coma (Geller et al. 1999) → NFW profile fits cluster density profile

Cluster and Infall Region Nearby Survey (CAIRNS) (Rines et al. 2003)

CIRS (Rines & Diaferio, 2006): 72 X-ray selected clusters with galaxy redshifts extracted from DR4-SDSS. Largest sample of clusters have been measured out to $\sim 3r_{200}$ → virial mass function → cosmological parameters consistent with WMAP (Rines et al. 2007, 2008)

Groups of galaxies: 16 groups – NFW profile confirmed (Rines & Diaferio, 2008)

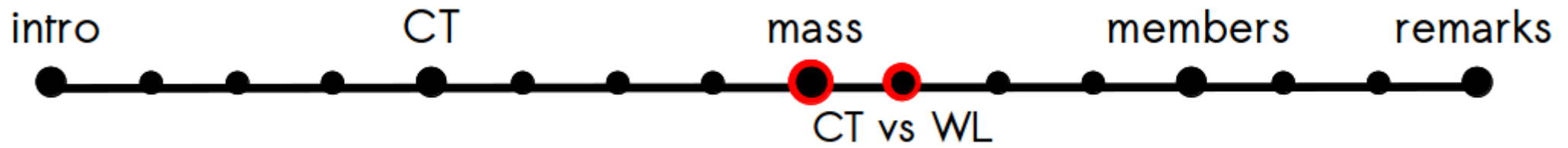
43 stacked clusters from 2dF (Biviano & Girardi, 2003)

Unrelaxed systems: Shapley superclusters (Reinsenegger et al. 2000, Davidzon et al. in prep), Fornax cluster (Drinkwater et al. 2001), A2199 (Rines et al. 2002)

Coma and CL0024 to measure w_{DM} (Serra & Dominguez, 2011)

Individual systems (Mahdavi et al. 2005; Lemze et al. 2009; Lu et al. 2010)

HeCS (Hectospec Cluster Survey; Rines et al. 2012): clusters in the redshift range $0.1 < z < 0.3$; more than 20,000 new redshifts; 17 clusters with WL mass profiles



caustics

lensing

requires

**wide-field redshift
survey**

**wide-field
photometric
survey**

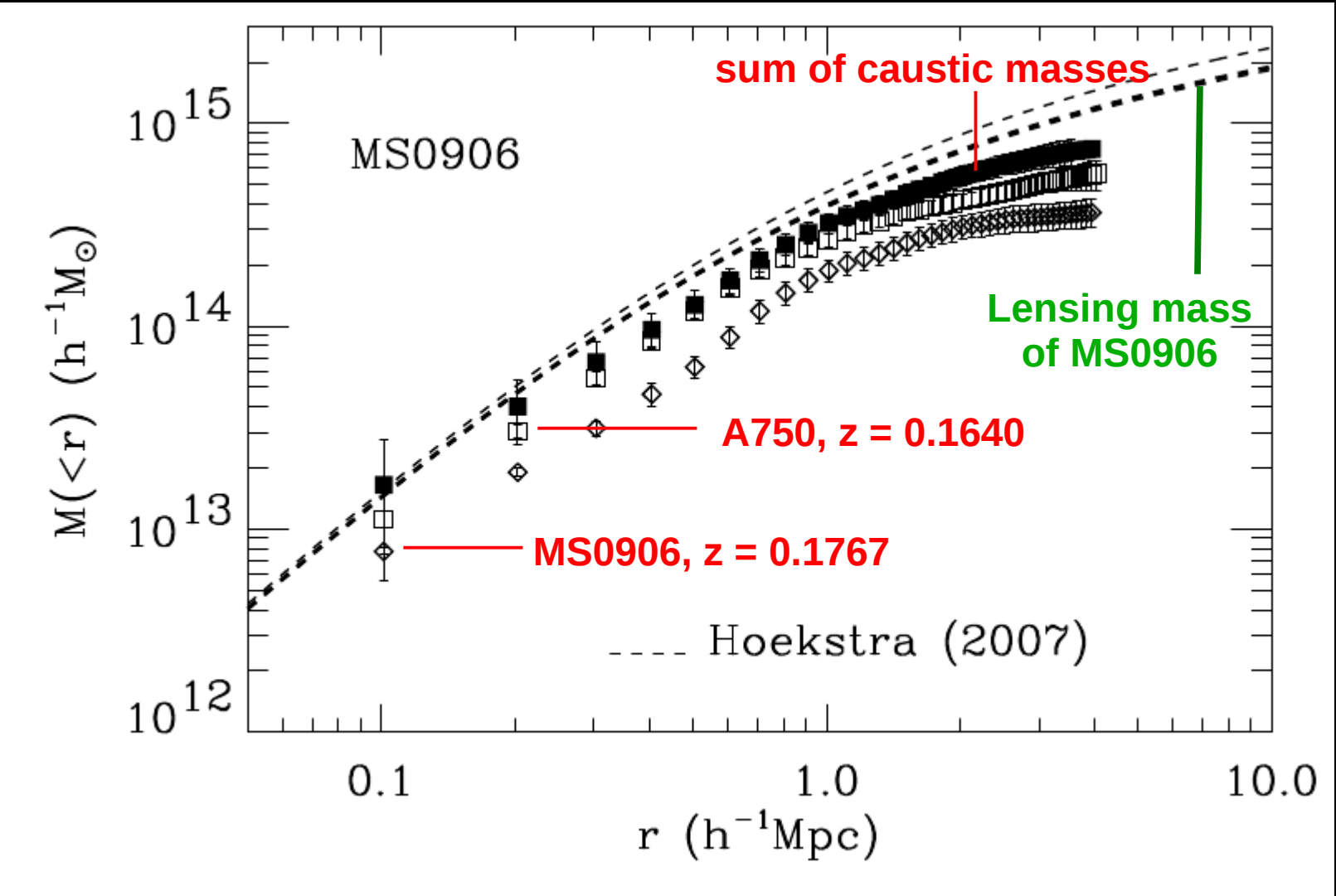
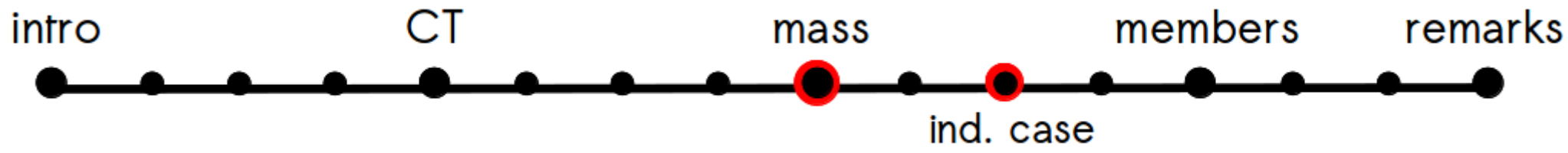
**sufficiently dense
survey**

**redshift where
signal is
sufficiently strong**

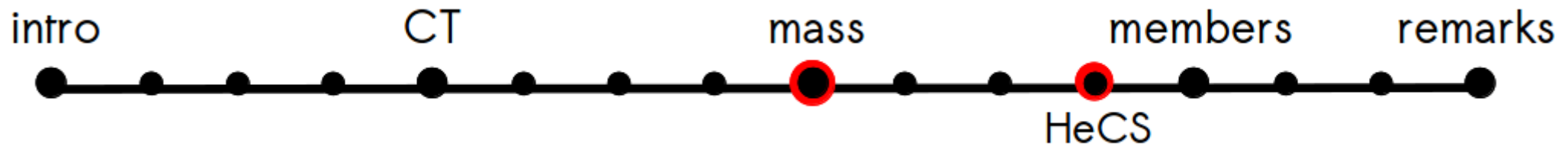
yields

**3D mass profile
affected by
projection**

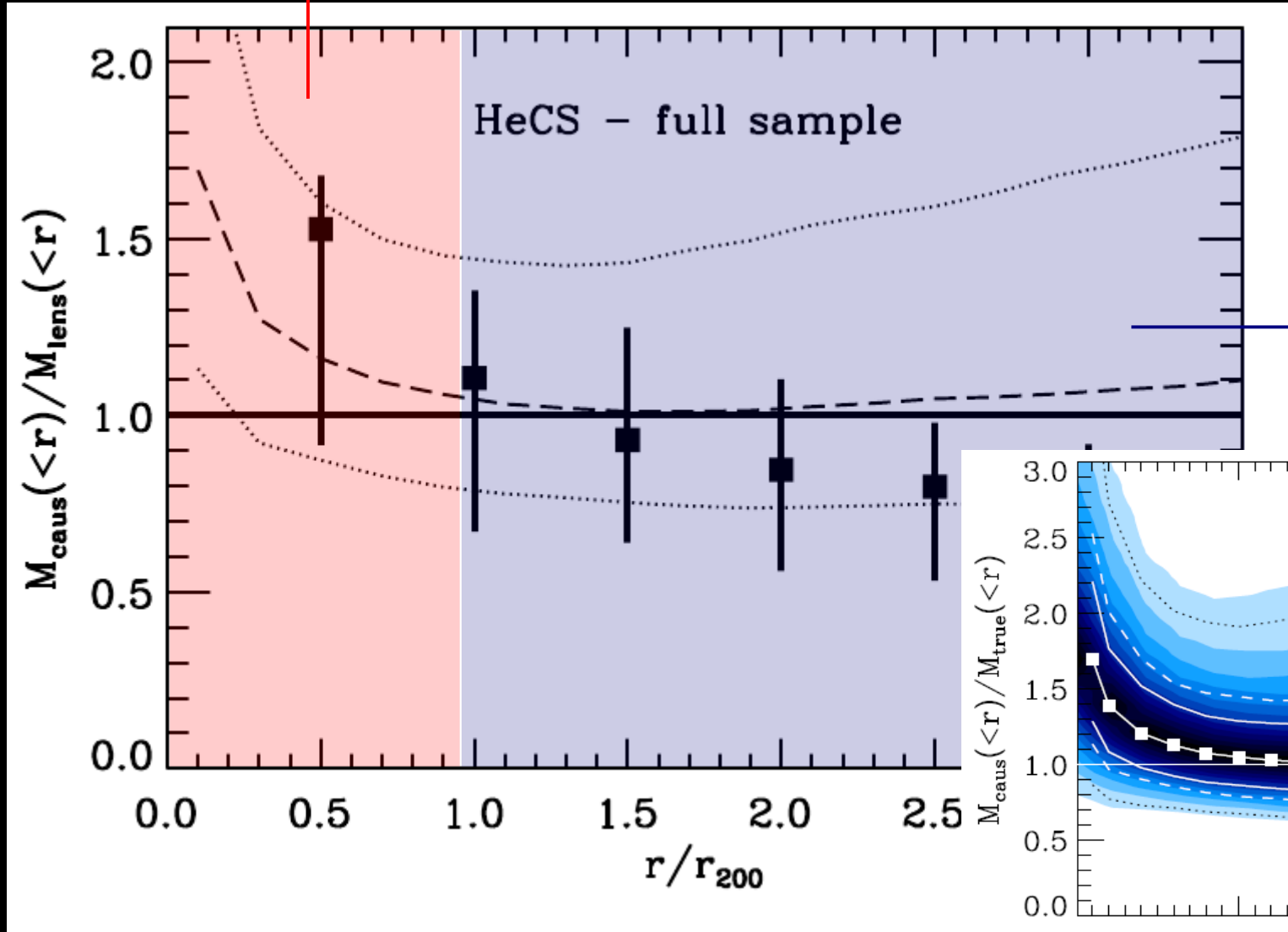
**projected mass
profile along the
line of sight**



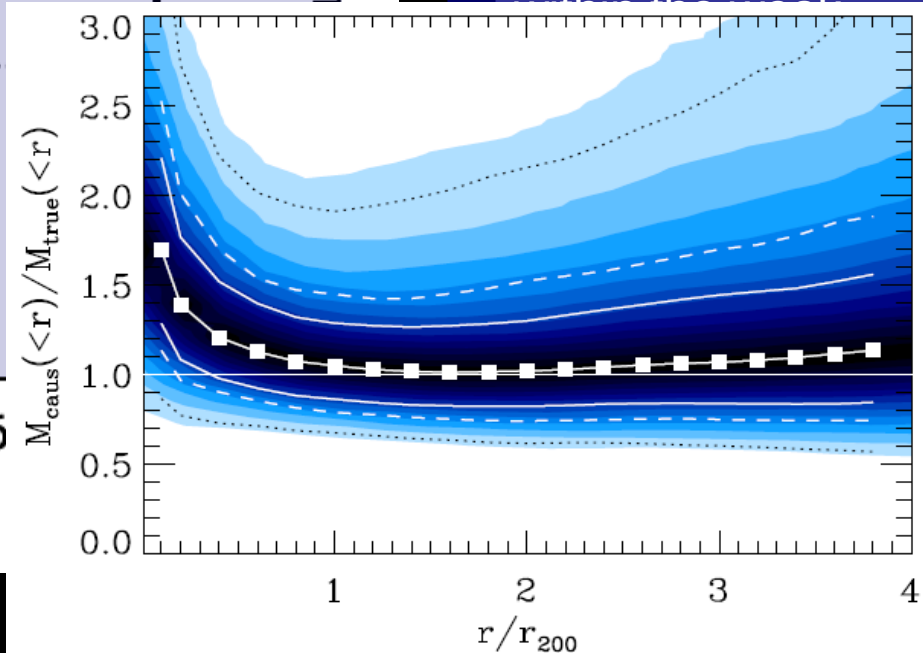
Geller et al. submitted

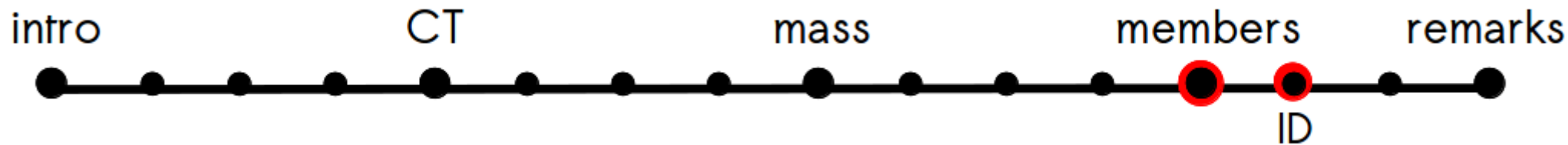


the caustic technique overestimates the mass in the inner regions



potential biases produced by large-scale structure superposed within the caustic





Membership

To study the dependence of properties on the environment we need to know whether a galaxy is member of a cluster

line-of-sight velocity

3σ clipping (Yahil & Vidal 1977): velocity distribution close to gaussian

gap method (Zabludoff et al. 1990; Beers et al. 1990)

adaptive kernel method (Pisani 1993)
probability density underlying the data

gaussian plus a constant function: fit to the velocity distribution (McKay et al. 2002)

+ projected radius

velocity of a galaxy depends on the gravitational potential profile of the cluster

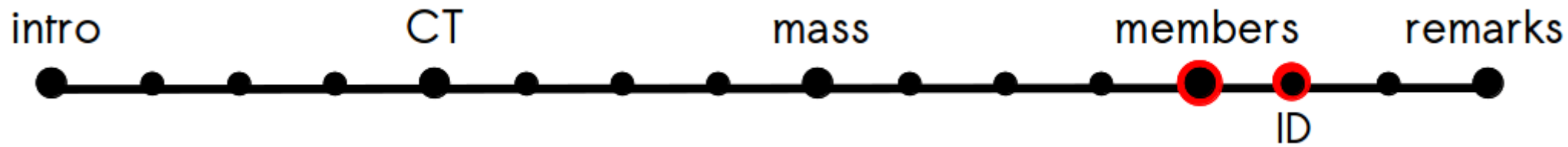
escape velocity profiles \rightarrow caustic technique

+ dependence of the VD on the projected distance to the center (Prada et al. 2003)

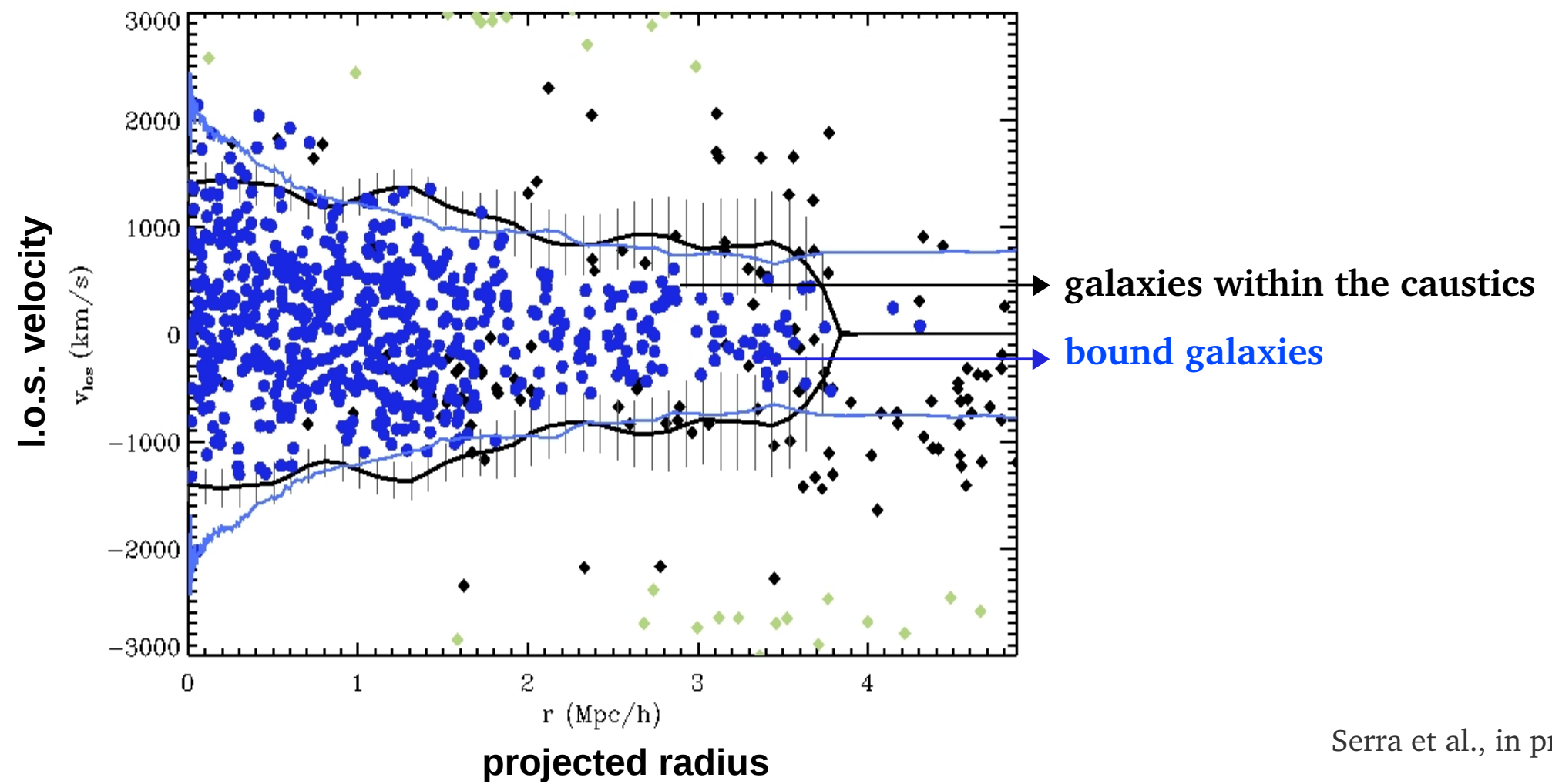
fit to σ_{los} according to the Jeans formalism ($\beta = 0$) (Lokas et al. 2006)

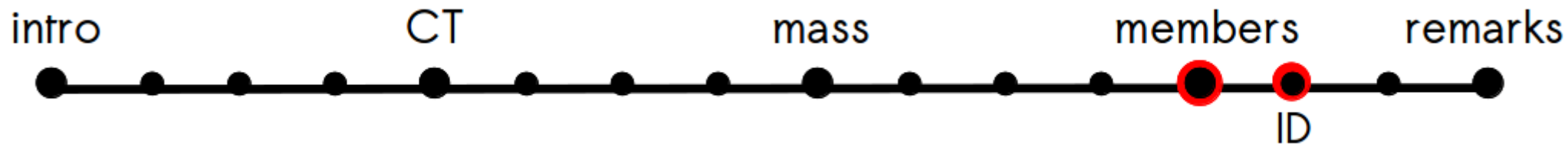
$v_{\text{max}}(R)$ from the mass distribution (den Hartog & Katgert, 1996)

boundary lines $\pm v_{\text{lim}}(R)$ on the velocity diagram (Wojtak et al. 2007)

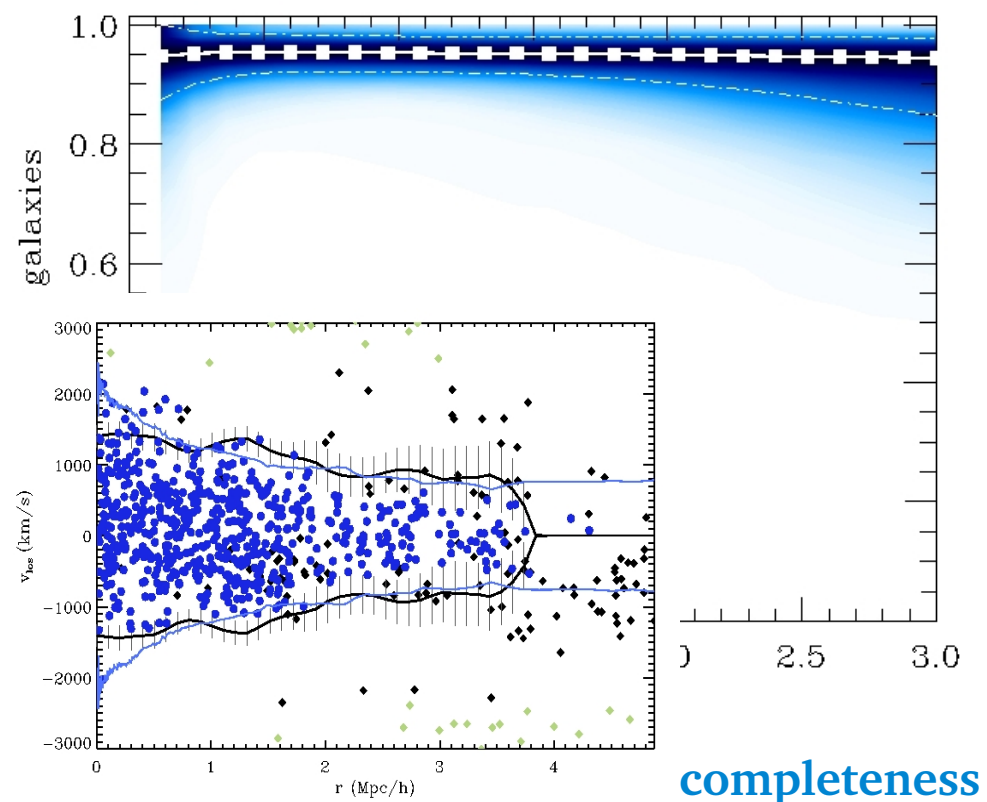


Membership

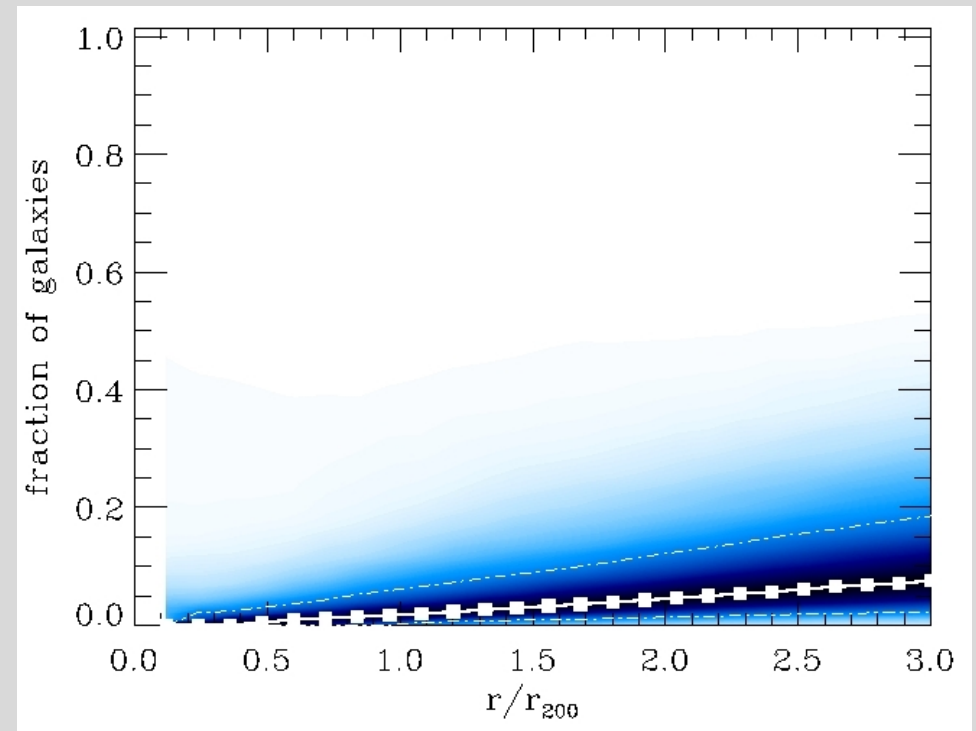




galaxies within caustics compared with bound galaxies

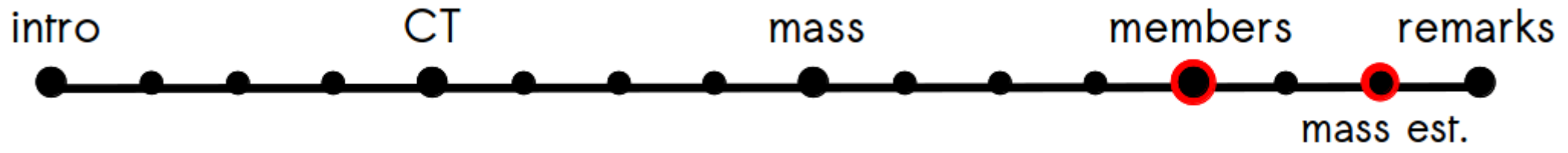


completeness

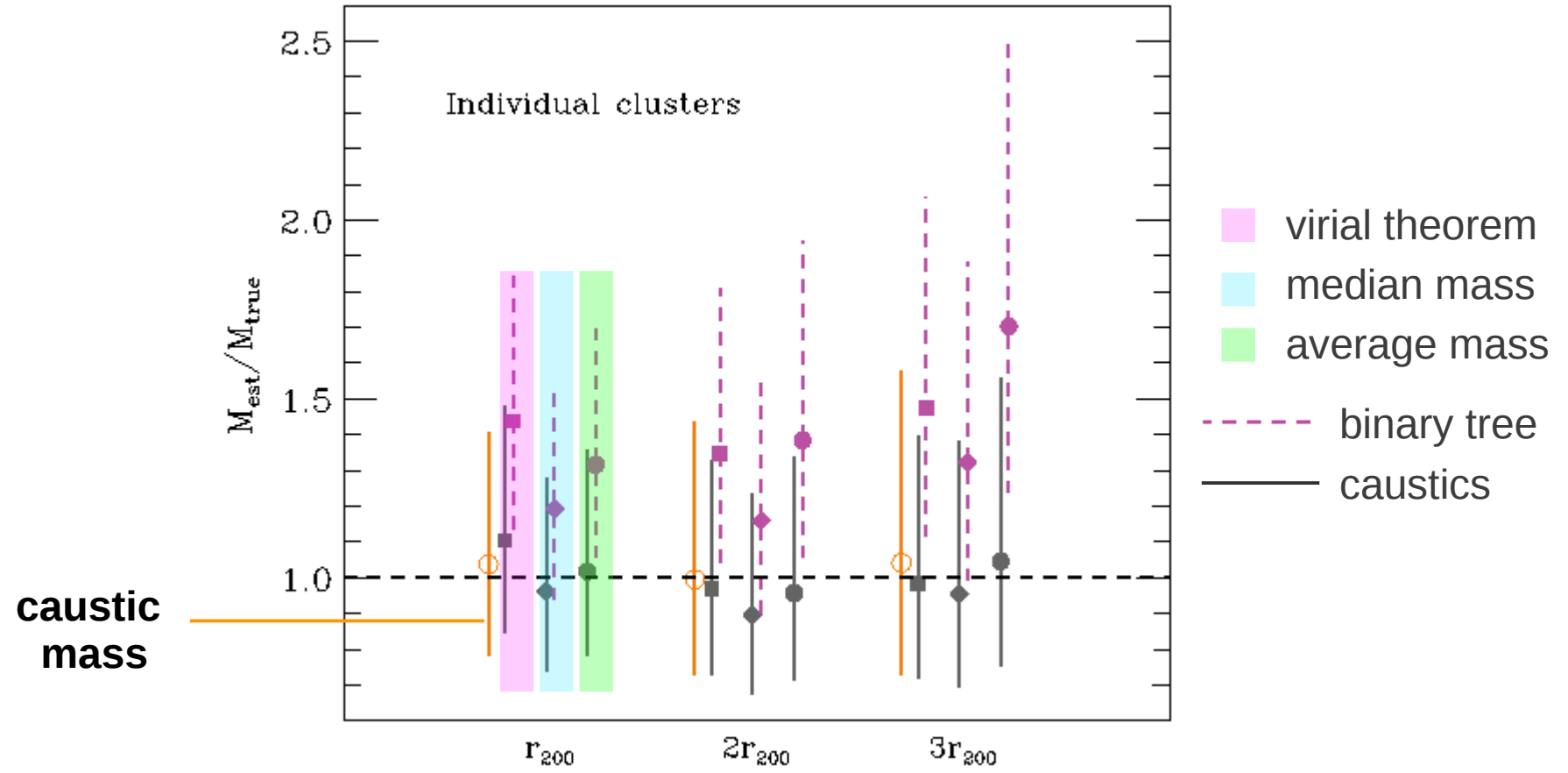


contamination

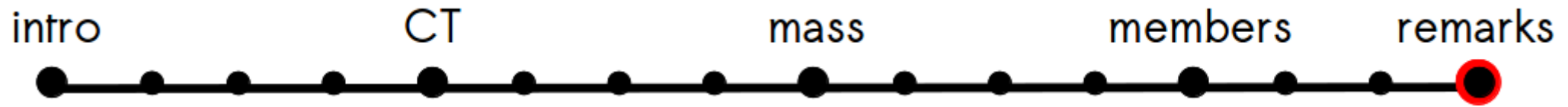
	-1σ	median	$+1\sigma$	-1σ	median	$+1\sigma$
r_{200}	0.921	0.956	0.984	0.005	0.020	0.066
$2r_{200}$	0.908	0.951	0.981	0.015	0.047	0.126
$3r_{200}$	0.875	0.947	0.980	0.027	0.080	0.193



Mass estimates



The caustic location performs systematically better in removing interlopers and, on average, the bias in the mass estimate is minimized



Remarks

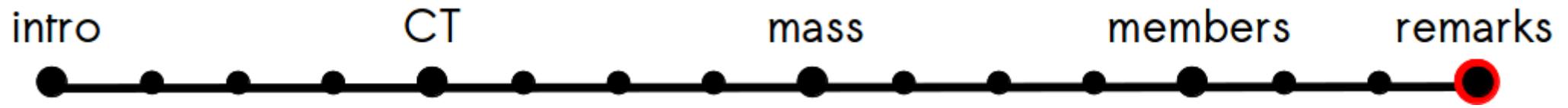
the caustic technique and gravitational lensing are the only two methods available to measure the mass profile of clusters beyond the virial radius without assuming dynamical equilibrium

~200 gxs in a field of 2.46 Mpc/h x 2.46 Mpc/h are enough to have an accurate escape velocity profile

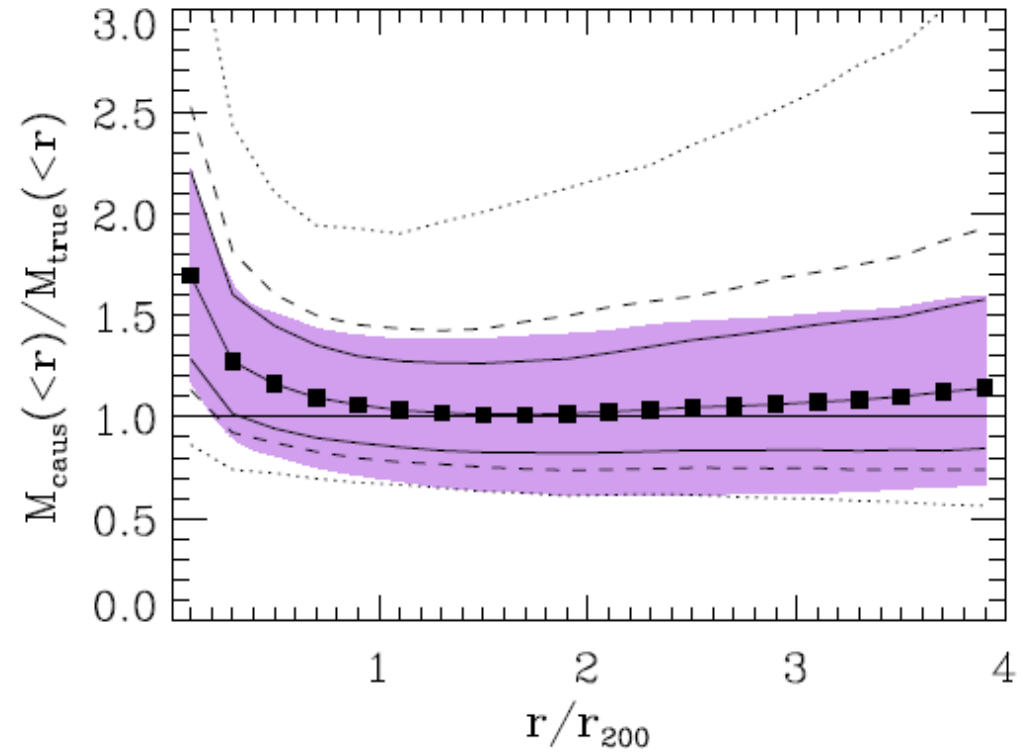
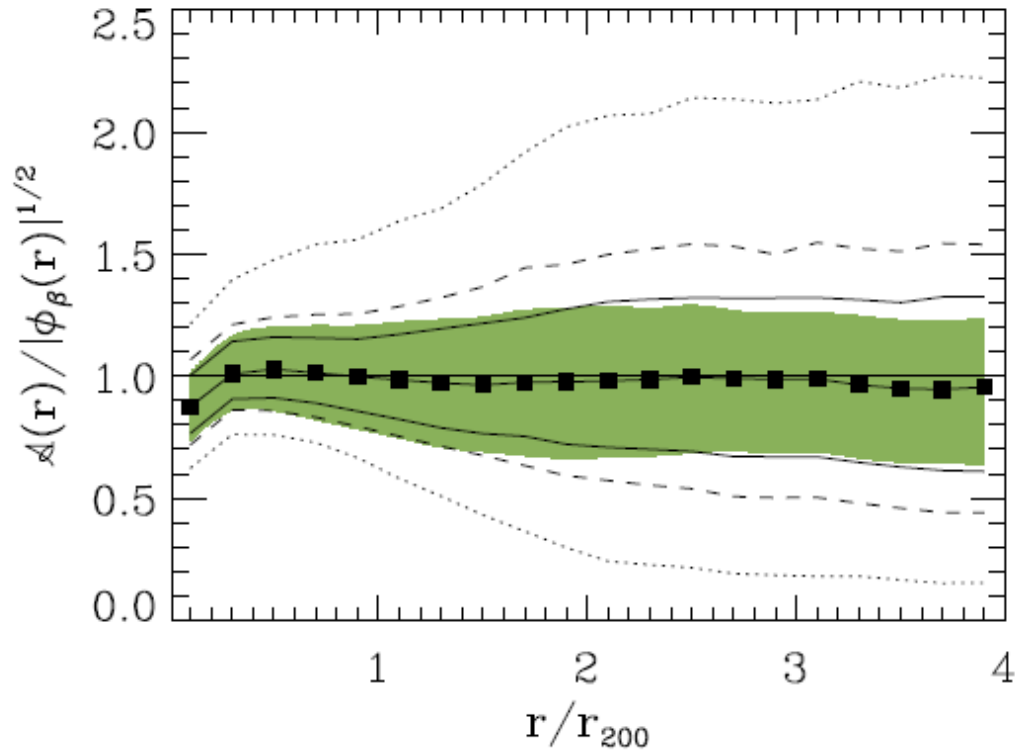
$F_{\beta}(r)$ is not constant in the inner parts of the cluster → overestimation of the mass

spread due to projection → but the formal errors account for that

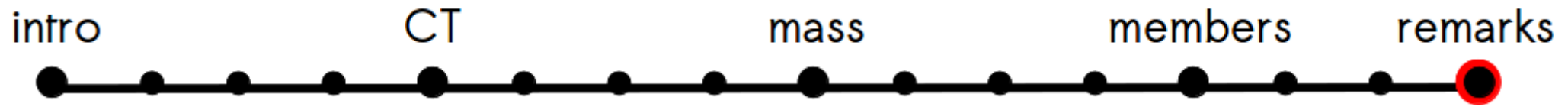
$$\delta M_i = \sum_{j=1,i} |2m_j \delta \mathcal{A}(r_j) / \mathcal{A}(r_j)|$$



Remarks



$$\delta M_i = \sum_{j=1,i} |2m_j \delta \mathcal{A}(r_j) / \mathcal{A}(r_j)|$$



Remarks

the applications of the caustic technique to a large sample of simulated clusters demonstrated that the escape velocity is recovered with $\sim 25\%$ $1-\sigma$ uncertainty and the mass profile with $\sim 50\%$ $1-\sigma$ uncertainty

the median ratio of the caustic and weak lensing mass profile in the 19 HeCS clusters is within the 68% confidence limits of the ratio between the true and caustic mass profiles derived from N-body simulations. At radii $< r_{200}$, the caustic approach overestimated the mass. Near the virial radius ($\sim 1.3r_{200}$) the profiles agree to $\sim 30\%$.

thank you!